MISCELLANEOUS PAPER CERC-90-3

US Army Corps of Engineers

INVESTIGATION OF SEISMIC WAVE GAGE ANALYSIS TECHNIQUES AND COMPARATIVE EVALUATION OF THE SEISMIC WAVE GAGE AT CHETCO RIVER, OREGON

by

Gary L. Howell, Joon P. Rhee

Coastal Engineering Research Center

DEPARTMENT OF THE ARMY
Waterways Experiment Station, Corps of Engineers
3909 Halls Ferry Road, Vicksburg, Mississippi 39180-6199

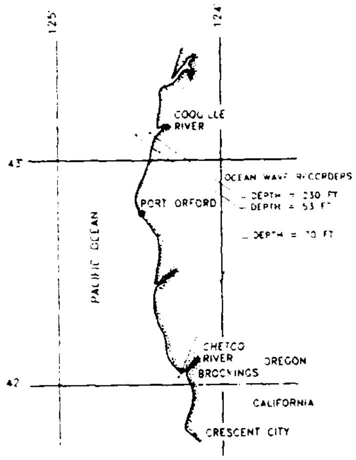

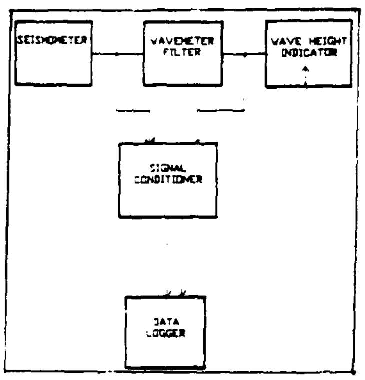

April 1990
Final Report

Prepared for US Army Engineer District, Portland
PO Box 2946, Portland, Oregon 97208-2946

Under Intra-Army Order No. E86850199 and E86860091

Unclassified
SECURITY CLASSIFICATION OF THIS PAGE

REPORT DOCUMENTATION PAGE

Form Approved
OMB No. 0704-0188

1a. REPORT SECURITY CLASSIFICATION
Unclassified

1b. RESTRICTIVE MARKINGS

2a. SECURITY CLASSIFICATION AUTHORITY

2b. DECLASSIFICATION/DOWNGRADING SCHEDULE

3. DISTRIBUTION/AVAILABILITY OF REPORT
Approved for public release; distribution unlimited.

4. PERFORMING ORGANIZATION REPORT NUMBER(S)
Miscellaneous Paper CERC-90-3

5. MONITORING ORGANIZATION REPORT NUMBER(S)

6a. NAME OF PERFORMING ORGANIZATION
USAEWES, Coastal Engineering Research Center

6b. OFFICE SYMBOL (If applicable)

7a. NAME OF MONITORING ORGANIZATION

6c. ADDRESS (City, State, and ZIP Code)
3909 Halls Ferry Road
Vicksburg, MS 39180-6199

7b. ADDRESS (City, State, and ZIP Code)

8a. NAME OF FUNDING/SPONSORING ORGANIZATION
USAED, Portland, OR

8b. OFFICE SYMBOL (If applicable)

9. PROCUREMENT INSTRUMENT IDENTIFICATION NUMBER

8c. ADDRESS (City, State, and ZIP Code)
PO Box 2946
Portland, Oregon 97208-2946

10. SOURCE OF FUNDING NUMBERS

PROGRAM ELEMENT NO.	PROJECT NO.	TASK NO.	WORK UNIT ACCESSION NO.

11. TITLE (Include Security Classification)
Investigation of Seismic Wave Gage Analysis Techniques and Comparative Evaluation of the Seismic Wave Gage at Chetco River, Oregon.

12. PERSONAL AUTHOR(S)
Howell, Gary L.; Rhee, Joon P.

13a. TYPE OF REPORT
Final Report

13b. TIME COVERED
FROM ______ TO ______

14. DATE OF REPORT (Year, Month, Day)
April 1990

15. PAGE COUNT
64

16. SUPPLEMENTARY NOTATION
Available from National Technical Information Service, 5285 Port Royal Road, Springfield, VA 22161

17. COSATI CODES

FIELD	GROUP	SUB-GROUP

18. SUBJECT TERMS (Continue on reverse if necessary and identify by block number)
Chetco River — Ocean waves
Measurement — Oceanographic instruments
Microseisms — Oregon

19. ABSTRACT (Continue on reverse if necessary and identify by block number)

High-energy wave environments have made the maintenance of traditional, in situ wave gages expensive and unreliable. An alternative to traditional gages is wave estimates based on microseismic measurements. Microseisms are small ground motions of relatively high frequency (compared with seismic activity) which are observed as a background noise on standard seismographs located close to the shoreline. It is generally accepted that microseismic activity is related to ocean waves and the amplitudes of microseisms often correlate with wave energy.

This work evaluates an existing wave meter system during summer wave conditions using digitally recorded data and computer analysis and investigates microseismic analysis techniques which might be useful to improve the seismic wave-measurement system. Both time

(Continued)

20. DISTRIBUTION/AVAILABILITY OF ABSTRACT
☒ UNCLASSIFIED/UNLIMITED ☐ SAME AS RPT ☐ DTIC USERS

21. ABSTRACT SECURITY CLASSIFICATION
Unclassified

22a. NAME OF RESPONSIBLE INDIVIDUAL

22b. TELEPHONE (Include Area Code)

22c. OFFICE SYMBOL

19. ABSTRACT (Continued).

domain and spectral analysis procedures were applied to seismic data. Correlation with both primary and doubled wave frequency components were investigated. Overall accuracy of the estimates is considerably less than that of in situ wave measurement instruments used currently by the US Army Corps of Engineers.

Accuracy and error sources are difficult to quantify without prior knowledge of the sea state. Accuracy may, however, be sufficient for certain operational purposes, where a need for a general sea-state estimate is all that is required and the ramifications of erroneous estimates are minimal.

PREFACE

The investigation was authorized by the US Army Engineer District, Portland (NPP), by Intra-Army Order E86850199 (21 November 1985) and E86860091 (29 November 1985). Mr. Eugene D. Pospisil and Mr. Steven A. Chesser were NPP Monitors for this study. Publication was supported by the Integrated Vertical Control and Sea State Work Unit, Dredging Research Program (DRP), sponsored by Headquaters, US Army Corps of Engineers. Mr. Andrew W. Garcia, Coastal Engineering Research Center (CERC), US Army Engineer Waterways Experiment Station (WES), was Principal Investigator. Mr. E. Clark McNair was DRP Program Manager.

This study was conducted and the report was prepared by Mr. Gary L. Howell and Dr. Joon P. Rhee, Prototype Measurement Analysis Branch (PMAB), Engineering Development Division (EDD), CERC. Work was performed under direct supervision of Dr. Dennis R. Smith, Chief, PMAB, Mr. William L. Preslan, Chief, PMAB, and Mr. Thomas W. Richardson, Chief, Engineering Development Division. General supervision was provided by Mr. Charles C. Calhoun, Jr., Assistant Chief, and Dr. James R. Houston, Chief, CERC.

The authors wish to thank Dr. Charles K. Sollitt, Oregon State University, for providing the comparison wave data.

COL Larry B. Fulton, CE, was Commander and Director of WES. Dr. Robert W. Whalin was Technical Director.

Contents

1 Introduction **1**

1.1 Objectives 2

1.2 Background 3

2 Experimental Data Collection **6**

2.1 Experimental Plan 6

2.2 Seismic Wave Meter Data Acquisition 6

2.3 Comparison Data 7

3 Data Analysis and Comparisons **9**

3.1 Evaluation of Estimates of Significant Wave Height by Existing Wave Meter 9

3.2 Evaluation of Period Estimates by Existing Wave Meter . . 10

3.3 Spectral Analysis of Raw Seismometer Data 11

3.4 Investigation of Primary Frequency Components in Seismic Spectra 12

3.5 Wave Height Estimates from Microseismic Spectra 14

4 Conclusions and Recommendations **16**

4.1 Wave Meter Accuracy 16

4.2 Improvements to the Seismic Wave Measurement System . 17

REFERENCES 18

FIGURES 1-36

APPENDIX A:
CORRELATION BETWEEN WAVE HEIGHTS AND ESTIMATES BY SEISMOMETER A1

Part 1

Introduction

The extreme wave climate of the Pacific Northwest and the need for nearshore wave data led to an investigation into the performance of the seismometer wave gage by the US Army Engineer Waterways Experiment Station's Coastal Engineering Research Center (CERC), Vicksburg, Mississippi, to evaluate its potential for satisfying wave data requirements of the US Army Engineer District (USAED), Portland, Oregon. Data were recorded simultaneously from the seismometer and from the output of the attached Oregon State University "wave meter" device during the summer of 1985 at Brookings, Oregon. Additional data were obtained for the same time periods from a directional wave gage installed by Oregon State near Brookings as well as other available data. The data were analyzed and compared, and various means of improving the analysis methodology were investigated.

Wave-height estimates from seismometer data can be shown to have a high correlation with actual sea states. Overall, however, the estimates by the seismometer are less accurate than required for wave statistics for US Army Corps of Engineers (Corps) project designs. Attempts to differentiate between local, nearshore wave conditions and offshore or distant conditions were partially successful, but additional comparison data and work are needed. Improvements in wave period estimates were successfully achieved, and reliable estimates of offshore dominant wave periods are probably obtainable.

A seismometer-based wave gage could be useful for wave estimates for operational purposes where the requirements for real-time, low-cost, reliable data would offset the limitations on system accuracy. Wave data from such a gage would infrequently be unavailable due to adverse seismic activity, and occasionally have large errors in estimates. There is, however, some indication that reliability during extreme wave events, which are of most interest, would be better than average. A seismometer coupled to a local microcomputer-based system could provide estimates via telephone, radio, or satellite links to Corps operational personnel or contractors. Development of such a system is well within the state of the art and would make use of the analysis techniques developed by this study.

1.1 Objectives

The USAED, Portland, Oregon, requires synoptic measurements of waves in the coastal and nearshore waters along the coast of Oregon to perform its various missions in planning, engineering, and operations. In the mid 1970's a system for sea-state measurement based on the principle of microseisms was developed by Oregon State University (OSU) and deployed at numerous Oregon coastal sites by the National Oceanic and Atmospheric Administration.

The CERC has undertaken an evaluation of the existing OSU seismometer wave meter to evaluate its accuracy and to determine what improvements, if any, could be made. In the first phase of this work, Thompson, Howell, and Smith (1985) reviewed the design of the wave meter system and analyzed the data manually using the wave-by-wave analysis method of CERC to compare with other wave data. The results for several winter storm periods indicated surprisingly good agreement for significant wave-height estimates, while period estimates often showed substantial disagreement. Several recommendations for improvement to the design of the wave meter were also made.

The objectives of the present work were to continue the evaluation of the existing wave meter system during summer wave conditions using digitally recorded data and computer analysis and to investigate microseismic analysis techniques which might be useful to improve the seismic wave-measurement system.

1.2 Background

The existence of small amplitude seismic waves of frequencies between 0.04 and 0.4 Hz has long been known. They have been detected by numerous observations throughout the world, mainly in coastal areas. Attempts to explain the mechanism of the high-frequency seismic noise have appeared in a number of publications. For general review, reference should be made to Darbyshire (1962) and Hasselmann (1963).

The theory that ocean surface gravity waves can cause seismic waves is well established analytically and supported by many experiments. It is well known that standing surface waves lead to the fluctuations of the mean dynamic pressure on the sea bottom. In this case, the pressure field has a component unattenuated by water depth, and the frequency is double that of the standing surface wave. This nonlinear (with respect to the wave amplitudes) theory was reviewed and applied to the problem of microseisms by Longuet-Higgins and Ursell (1948) and again later by Longuet-Higgins (1950) with a complete microseism generation theory. Cooper and Longuet-Higgins (1951) reported a wave tank experiment on the pressure variations due to standing waves. *Although Longuet-Higgins' explanation of micro*seisms is based on the precondition of standing waves and has not always been supported by experiments (see Donn(1952)), many observations have confirmed the relationship between the frequencies of ocean waves and microseisms and thus supported this theory (see Deacon (1947), Dinger and Fisher (1955), Carder (1955), and Haubrich, Munk and Snodgrass (1963)).

Zopf, Creech and Quinn (1976) suggested a method for ocean wave measurements based on seismic recordings, employing the generation theory of Longuet-Higgins (1950). The method assumed that relationships between amplitudes of the elastic deformation of the sea bottom and the pressure caused by ocean waves are linear and thus the amplitudes of ocean waves can be measured by an empirical calibration curve representing a relationship between amplitudes of microseisms and ocean waves. This simplified hypothesis ignores all the complications of microseismic generation, propagation, and sensing. However, the application of the linear assumption appeared to be somewhat successful in estimating nearshore waves along the Oregon coast as reported by Creech (1981) and Thompson, Howell and Smith (1985).

The OSU wave meter applies a linear, ω^{-3} , transfer function to the seismometer velocity signal and displays the resulting voltage as a wave amplitude. The voltage is empirically calibrated with a square root law, arising from the Longuet-Higgins' generation theory. Ocean wave periods are assumed to be exactly double the observed periods of the wave meter output.

In the present work, we also investigated two potential improvements to the simple assumptions of the wave meter. First, the use of spectral analysis of the seismometer signal to improve estimates of the dominant period of ocean waves was considered. Second, the use of the primary microseismic spectrum was investigated to assist in correctly estimating the dominant period, and to determine if estimates of nearshore waves could be separated from offshore waves. Since the primary interest of the Corps is for sea conditions in coastal areas rather than in deep water, the later effort was considered important. Nearshore wave characteristics often vary considerably from those in deep water because of the complexities of shallow-water wave propagation, refraction, diffraction, reflection, and shoaling. The local bathymetry, wind and currents, as well as the frequency and directional spectrum of the offshore waves affect the variations. For this reason, a direct measurement of the shallow-water waves is usually required.

The original design of the wave meter relies on manual strip chart analysis to determine wave periods. An obvious improvement would be the digitizing output signals from the wave meter and the analyzing time-series periods by a computer. This approach has been implemented on an experimental basis as part of the work reported here. The period was estimated using an average zero-crossing algorithm to approximate the manual analysis method. This time-domain analysis, however, can only be expected to yield period estimates comparable to measurements from wave spectra, if the spectral shape of the seismometer signal is similar. Longuet-Higgins' analysis (1950) was based on monochromatic, deterministic waves and not a random sea surface. Hasselmann (1963) derived several cases of spectral shape of the seismic response, which were not, in general, the same as the wave spectrum. Kadota and Labianca (1981) proposed that, in deep water, the spectral shape of the seismic response is dependent only upon the swell portion of the surface wave spectrum, and the random phase, wind-sea makes no contribution. Their formulation predicts a spectral shape of the seismic reponse which is different from the sea-surface spectrum.

Darbyshire (1950) and Haubrich, Munk and Snodgrass (1963) presented seismic spectra having a peak at the frequency which is twice that of dominant ocean wave frequency. Especially, Haubrich, Munk and Snodgrass (1963) pointed out the correlation between the dispersive changes of the seismic and ocean wave peak frequencies with time.

Therefore, it is reasonable to propose that a seismic wave meter system should use spectral analysis to determine period estimates rather than a zero-crossing analysis. In the present work, the use of the peak of the seismic spectrum is examined to estimate the spectral peak of ocean waves. Following the deterministic analysis of Longuet-Higgins, the peak of the wave spectrum should be one half the frequency of the peak of the seismic spectrum. Under the more general assumptions of Hasselmann (1963) and Kadota and Labianca (1981), the ratio of spectral peaks could vary. For a swell-dominated sea, such as often characterizes the high sea states near the Oregon coast, the ratio should closely approximate two.

The "primary" spectrum of microseisms refers to small amounts of energy which appear at the same frequency as nearshore ocean waves. This sort of longer period seismic wave is also well known from experiments, for example, Pomeroy (1959) and Oliver (1962). These seismic waves appear to have the same period as ocean waves. The spectral results of microseisms presented by Haubrich, Munk and Snodgrass (1963) showed that the microseisms recorded near San Diego, California, had a primary frequency peak, of small intensity, but clearly related to ocean swell. Thus, these earlier studies accordingly suggested a theory that such seismic activities must be due to local water waves impacting a coastline. This theory was extended to an extensive mathematical development by Hasselmann (1963).

The existence of the primary spectrum related to nearshore waves could provide a mechanism to solve one of the problems of the existing measurement system of seismic waves. That is the inability to separate seismic responses to ocean waves of interest locally from those to other sources, for example, ocean waves at a great distance from the seismometer. A secondary application could be to provide assistance in estimating the period of the local sea state.

Part 2

Experimental Data Collection

2.1 Experimental Plan

The experimental plan was conceived as a minimum cost effort to acquire data sufficient to examine the proposed improvements to the seismic-wave measurement system. An existing OSU seismic-wave meter system at the Chetco River Coast Guard Station near Brookings, Oregon, was retrofitted with a digital data logger. The data acquisition period was planned to coincide with wave measurements by other groups in order to provide comparison data. Figure 1 shows the locations of the various measurement sites.

2.2 Seismic Wave Meter Data Acquisition

The seismic wave meter is composed of a Teledyne-Geotech Model SL-210 portable seismometer designed for geophysical surveys. As used with the wave meter, it is adjusted for critical damping with a natural period of about 18 sec. The output of the seismometer is connected to a preamplifier and filter which produces the wave meter output. For this experiment the output of the seismometer and the filter were simultaneously recorded by a Sea Data Model 1250 digital data logger. The signals were tapped from the wave meter circuitry which remained in operation. They were then amplified and scaled to within the range of the data logger by a signal conditioner composed of adjustable instrumentation amplifiers. Figure 2 is a block diagram of the data acquisition system. Data from both channels were sampled at 2 Hz for 17 min every 4 hr.

The wave meter is normally empirically calibrated to observed wave conditions at each site. The calibration for the wave meter voltage recorded by the data logger was determined by adjusting the wave meter zero control over the operating range of the meter indicator, while simultaneously measuring the voltage input to the data logger and manually recording the wave-height indication on the meter. Since the meter scale is used to provide the square root dependency of the output, the resulting curve is a bipolar quadratic. Figure 3 is a plot of a curve fit through the measured values and is the calibration used for the wave-meter data analysis. It could not be established that the wave meter site at Chetco River had ever been formally calibrated to observed wave conditions. No recalibration or adjustment of the "K" value had been performed in the recent memory of personnel familiar with the installation. The seismometer and electronics, however, had been regularly maintained and were in good operating condition both during and after the experiment. Because of the question about the absolute calibration, interpretation of the magnitudes of comparison data should be done in a relative sense.

No attempt was made to provide an absolute calibration of the raw seismic signal. The velocity signal was amplified by an arbitrary gain to provide sufficient sensitivity to microseisms. The amplified signal was filtered by a low pass, 6 pole, Butterworth filter with a corner frequency of 1 Hz. The resulting voltage was recorded by the data logger.

2.3 Comparison Data

For comparison, wave data of shallow water were provided from an acoustic current meter located in 78 ft of water just offshore from the seismometer site. This gage was part of a current meter deployment by Dr. Charles K. Sollitt, OSU, under the sponsorship of the Portland District.

Since data from OSU were not always available during comparison periods, supplementary comparison sites were also used. Near Coquille River, a waverider buoy in deep water and an S_{xy} array in shallow water are operated for the Corps, Field Wave Gaging Program by the Scripps Institute of Oceanography (SIO). Although these gages are located some distance from the Chetco seismometer, they are exposed to similar offshore wave conditions (Figure 1).

Part 3

Data Analysis and Comparisons

3.1 Evaluation of Estimates of Significant Wave Height by Existing Wave Meter

Figures 4 through 9 show the time-series of significant wave heights from the seismometer and comparison gages. The significant wave heights furnished by SIO and OSU were calculated from spectral estimates as four times the square root of zero moment. The significant wave heights for the seismometer were calculated by averaging the highest one-third waves in the time domain.

In Figure 4, the periods from Julian day (J.D.) 195 through 198 show comparable estimates from both the seismometer and the closely located OSU gage. From J.D. 198 through 214 (Figure 5), however, the estimates begin to diverge widely. In fact, the seismometer data show better agreement with the deepwater buoy data of SIO during this period than the closer, but shallower data of OSU.

Again, during two moderate storms in August (Figure 6), it can be seen that the seismometer estimates follow the general pattern of the deepwater buoy. Unfortunately, Chetco River data were not available during this time period. While a systematic difference of the estimates would not be surprising given the questions about calibration of the seismometer gage, the seismometer appears to overestimate the wave heights during the first storm and underestimate during the smaller second storm. Without comparison data, it cannot be ruled out that the area near the seismometer responded differently to the two storms.

Figures 7 and 8 show results from two winter storms. Again Chetco River data were not available, but good agreement can be seen in the shape of the variation of significant wave heights during the course of the storms, except for a systematic difference in the amplitude.

3.2 Evaluation of Period Estimates by Existing Wave Meter

The results for time-series of wave periods are presented in Figures 10 through 15. Wave periods for OSU and SIO estimates represent the period at which a maximum density occurs in the wave spectrum. For the wavemeter estimates, the average zero-crossing period of the highest one-third waves was calculated to be consistent with previous manual methods used. The seismometer data are plotted without applying the constant multiplier of two. The wave periods obtained from OSU and SIO may be used to estimate the significant wave periods by using one of the experimental formulae (see Goda 1974). However, this would result in only slight changes in their values.

These plots show comparisons of the period estimates from the same data sets as the significant wave-height comparisons. Based on traditional wave meter analysis procedures, the wave meter period should be one half the wave period.

The periods of typical low summer waves such as those in Figures 10 and 11 show some events where the wave meter estimates are reasonably close to the periods measured by the OSU gage. There are, however, long sequences where the seismometer wave meter appears to be responding to a period quite different from those of the OSU gage. Unlike the wave-height comparisons, the period estimates do not show any strong correlation with the SIO deepwater buoy. During the storm events shown in Figures 12 through 14, period estimates come much closer to one half of the observed wave periods. Although the apparent correlation is much stronger, there are still several segments when the estimates diverge sharply. Again, since shallow-water data near the seismometer were not available, local effects could not be evaluated.

3.3 Spectral Analysis of Raw Seismometer Data

Figures 16 through 20 show smoothed spectra of the raw seismometer velocity signal. The three-dimensional plots are composed of a sequence of autospectra, one for each 17-min data record. The raw seismic data include the same measurement periods as the data from the wave meter presented in the last section.

The plots from the July 1985 measurements show dominant peaks at the secondary frequencies. The shape of the spectra, however, is quite broad and contains multiple peaks. Because of the difficulty in applying peak detection algorithms to spectra with such a high variation, peak frequency estimates were computed at the centroid of the spectra, or the period of the first moment.[1]

It is clear from the plots that an energetic secondary spectrum exists for every wave record, both for the small wave heights during the summer conditions, and for the storm events in August 1985 and March and April 1986 (Figures 18 through 20). A microcomputer analysis program running in real-time should be able to robustly compute spectra from a raw seismometer signal and compute period estimates from the centroid of the spectrum.

Figures 21 and 22 show the results of period calculations from the spectra together with SIO estimates for the August storm. The general evolution of the seismic period estimates follows closely the measured data, especially the deepwater buoy. The variations in period show the expected dispersive effects of storm wave arrival which has been noted in previous seismic investigations (Haubrich, Munk and Snodgrass (1963)).

Figures 23 and 24 show a scatter diagram of periods estimated from

[1]

$$\overline{f} = \frac{\int f S(f)\, df}{\int S(f)\, df},$$

where $\overline{f}$ = peak frequency estimate, f = frequency, and $S(f)$ = power spectral density.

the seismic spectra versus the comparison periods for both the deepwater data and shallow-water data from SIO. The plot includes all data points from both the winter and summer cases. The grouping of the points is quite good, especially with the deepwater data. The slope of the linear regression line through the points is 0.47. The scatter of points with the shallow-water comparison data is not as tight, and the slope of the linear regression line is 0.42. Again, the distance of this shallow-water data from the seismometer site could account for these differences.

To examine further the implications of using a simple double-frequency assumption to estimate wave period from the seismometer spectrum, in Figures 25 and 26 we plot a histogram of the ratio of comparison data to the seismometer spectral peak period. For the deepwater data, the mean value is 2.16 with a standard deviation of 0.27. When the ratio is computed with the shallow-water data, the mean is 2.37, and the standard deviation is 0.3.

3.4 Investigation of Primary Frequency Components in Seismic Spectra

Close inspection of the microseismic spectral plots for the summer data (Figures 16 through 18) show clear evidence of small amounts of energy at frequencies lower than the secondary frequency peaks. The energy appears around 0.15 Hz, or close to the 6- to 7-sec periods reported from the SIO deepwater buoy as shown previously in Figures 10 and 11. Since this frequency is also approximately one half the peak periods estimated from the secondary frequencies, it may be concluded that these peaks are primary frequency energy. It is also interesting to observe that the relative amount of energy in the primary peaks does not always correlate with the energy in the secondary peaks, supporting the hypothesis of previous investigators that different physical generation processes are involved in the primary and secondary energy. The fact that primary spectral energy appears to be present much of the time, even in relatively mild, summer sea conditions is also an important observation.

Figures 27 and 28 are expanded portions of the spectra from part of the July data. At this scale, energy in the period range around 0.06 Hz, which appeared flat in the previous plots, is clearly visible. Returning to the comparison between seismometer period estimates and the OSU gage near Chetco River shown in Figures 10 and 11, there was a time starting about July 16 where the seas measured by the pressure gage appeared to come under the influence of a swell of about 17 sec. During this period the estimates from the wave meter became somewhat confused. It does appear in comparing Figures 27 and 10 that observable energy at the 16- to 17-sec period in the seismic spectrum correlates with the times that the pressure gage was showing similar periods. Also during this period, the SIO deepwater buoy continued to show the periods of the wind-sea.

Figure 29 is a single spectrum of the seismometer signal from July 19, when the swell part of the primary spectrum was particularly energetic. This plot shows some of the opportunities as well as the potential problems in considering the primary spectrum. Since the sea state was composed of both a swell component at 17 sec and a wind-sea at about 7 sec, these components can be identified as having energy in both the primary and secondary frequencies. Unfortunately, the secondary swell energy, theoretically falling at 0.12 Hz, comes very close to the primary wind-sea at 0.14 Hz. This could present problems in separating the contributions without prior knowledge of the spectrum.

Turning to the case of winter data, the spectral densities of the secondary frequencies are more than an order of magnitude larger than the the summer spectra. In most cases any primary energy is completely obscured at the plotting scale of Figures 18 through 20. For example, Figure 30 shows a single spectrum plot from March 11 in a form similar to Figure 29. No primary energy is visible. Looking at the August storm, Figure 31 shows an expanded scale of the spectrum from August 2. Again very little primary energy is visible. Eight hours later, however, Figure 32 shows a peak has developed around 0.07 Hz. This corresponds with the development of the storm and the gradual shift towards a swell period as measured by the SIO buoy as shown in Figures 6 and 12. The same development can be seen for the March storm in Figures 33 and 34. The shape of the primary spectrum in Figure 34 looks remarkably similar to a wave spectrum.

3.5 Wave-Height Estimates from Microseismic Spectra

Spectral analysis of the raw seismic signal would permit estimation of significant wave heights using the same assumptions and the equivalent signal processing as employed by the linearizer circuit of the wave meter. A digital low pass filter with the same response characteristics could be applied and the results either analyzed in the time domain as in the evaluation section of this report, or equivalent estimates could be computed based on the zero moment of the filtered microseismic spectra. In any case, the results would be the same as previously presented.

Potential improvements to wave-height estimates could be pursued by attempting to evaluate the energy of the primary and secondary frequencies. It is hoped that the primary frequencies may assist in separating the effects of nearshore and distant seismic activity. Some encouragement was found for the case of periods above. Unfortunately, too little nearshore comparison data were available to evaluate use of the primary frequency energies. Simultaneous offshore, nearshore, and seismometer data for a long measurement period would be required. Given that adequate correlation between primary peak energy and local significant wave height could be established, applying this in a wave measurement system would present additional difficulties. Because of the very small energies of the secondary peaks, and the possible occurrences of overlap as noted above, algorithms for separation of the spectra would be more difficult than the relatively straightforward computations used for the period estimates. The acquisition of the needed data and the development of such algorithms could present a useful path for future work.

For a simple analysis procedure based on the microseismic spectrum, the following was considered. Remembering that the primary spectrum contributes very little energy to the total, some simple comparisons were computed. The total energy of the raw seismic spectrum was computed as the square root of the zero moment. Figures 35 and 36 show the square root of the total energy plotted against observed wave height for both deepwater and shallow-water data from SIO. For the deep-water scatter diagram, the points fall reasonably close to a straight line, except for a number of records when the wave height was grossly underpredicted. Because of the limited amount of comparison data close to the seismometer, it is difficult to make conclusions based on these results, but the agreement does not seem to be significantly worse than that obtained from the present wave meter method. Of course, use of either of these methods would still rely on the site-specific calibration of the curve as is presently the case for the wave meter.

Part 4

Conclusions and Recommendations

4.1 Wave Meter Accuracy

The results of comparing significant wave height estimates from the existing wave meter system for summer wave conditions were not as favorable as the results previously reported for winter storms only. Results from the small amount of winter data compared here show greater correlation than from the summer data, but large errors existed in actual estimates. Better site-specific calibration of the seismometer at Chetco River could reduce these errors. As in the previous report, period estimates frequently had large errors.

A limited amount of comparison data was available for local wave conditions near Chetco River. No local data were available for the winter comparison periods. Based on this limited set of summer data, the wave meter estimates appear to be more strongly influenced by distant deepwater conditions than local conditions. For cases of large swell-dominated storms, local conditions may closely parallel distant conditions.

The seismic system operated reliably during the entire data acquisition period and provided continuous data except during periods of geoseismic activity. Periods of seismic activity which prevent wave estimates can last from hours to days.

4.2 Improvements to the Seismic Wave Measurement System

Directly digitizing and processing the raw seismic signal are feasible. Spectral analysis of the seismic data improves estimates of wave period. Initial approaches should use the energetic secondary frequencies to estimate the peak period and then use a constant multiplier of two to estimate the ocean wave period. Additional comparison data and investigation may allow the use of the primary frequency to assist in separating the periods at the local site from more distant conditions. Estimates of significant wave height can be made using a digital system. These estimates should be at least as good as the existing wave meter.

It is well within the state of the art to design and construct a ruggedized microcomputer system capable of digitizing and processing the seismometer signal in real-time. Estimates of wave height and period, along with quality control checks, could be produced using analysis methods similar to those reported here. Wave estimates could be stored internally and transmitted to a central site via telephone, radio, or satellite communications technology. The microcomputer system could be constructed to withstand a severe marine environment. The seismometer itself, however, requires a temperature-controlled environment. The microcomputer system could be designed such that its power consumption would be low enough to allow solar-powered operation. The power required to temperature control the seismometer would be the limiting factor on total system power consumption. In most cases, the seismometer heating requirements would require connection to an electric utility or some other source of accurately controlled heat. The development of real-time, robust versions of the analysis programs would represent the major development cost of the system.

References

Bodvasson, G. M. 1975. Ocean Wave Generated Microseisms at the Oregon Coast. MS Thesis, Oregon State University, Corvallis, OR.

Carder, D. S. 1955. Microseisms at Bermuda. *Tran. Amer. Geophs. Un.*, **36**, pp. 843-854.

Cooper, R. I. B. and M. S. Longuet-Higgins. 1951. An experimental study of the pressure variation in standing waves. *Proc. Roy. Soc. London*, **A206**, pp. 424-435.

Creech, H. C. 1981. Nearshore wave climatology, Yaquina Bay, Oregon (1971-1981). *Oregon State University University Sea Grant College Program*, Oregon State University, Corvallis, OR.

Darbyshire, J. 1950. Identification of microseismic activity with sea waves. *Proc. Roy. Soc. London* **A202**, pp. 439-448

Darbyshire, J. 1962. Microseisms, in *The Sea*, **1**, *Physical Oceanography*, edited by M. N. Hill, pp. 700-719, Interscience, N.Y.

Deacon, G. E. R. 1947. Relation between sea and microseisms. *Nature*, **160**, pp. 419-421.

Dinger, J. E. and G. H. Fisher. 1955. Microseism and ocean wave studies at Guam. *Tran. Amer. Geophs. Un.*, **36**, pp. 262-272.

Donn, W. L. 1952. An investigation of swell and microseisms from the hurricane of September 13-16, 1946. *Trans. Amer. Geophs. Un.*, **33**, pp. 341-344.

Goda, Y. 1974. Estimation of wave statistics from spectra information. *Proc. Int. Symp. on Ocean Wave Measurement and Analysis*, ASCE, New Orleans, pp. 320-337.

Hasselmann, K. 1963. A statistical analysis of the generation of microsesms. *Reviews of Geophysics* **1**, No. 2, pp. 177-210.

Haubrich, R. A., W. H. Munk and F. E. Snodgrass. 1963. Comparative spectra of microseisms and swell. *Bull. Seism. Soc. Amer.*, **47**, pp. 27-37.

Kadota, T.T. and Frank M. Labianca. 1981. Gravity-wave induced pressure fluctuations in the deep ocean. *IEEE Journal of Ocean Engineering*, **OE-6**, No. 2.

Longuet-Higgins, M. S. 1950. A theory of the origin of microseisms. *Phil. Trans. Roy. Soc. London,* **A243**, pp. 1-35.

Longuet-Higgins, M. S. and F. Ursell. 1948. Sea waves and microseisms. *Nature,* **162**. pp. 700.

Oliver, Jack. 1962. A worldwide storm of microseisms with periods of about 27 seconds. *Bull. Seism. Soc. Amer,* **52**, No. **3**, pp. 507-517.

Pomeroy, Paul. 1959. Background and storm microseisms in the period range 11-12 seconds. *Journal of Geophys. Res.*, **64**, pp. 1120.

Thompson E. F., G. L. Howell and J. M. Smith. 1985. Evaluation of Seismometer wave gage and comparative analysis of wave data at Yaquina and Coquille bays, Oregon. *USAE Waterways Experiment Station, Miscellaneous Paper* **CERC 85-12**.

Zopf, D. O., H. C. Creech and W. H. Quinn. 1976. The wave meter: A land based system for measuring nearshore ocean waves. *Marine Technology Soc. Journal,* **10**, No. 4, pp. 19-25.

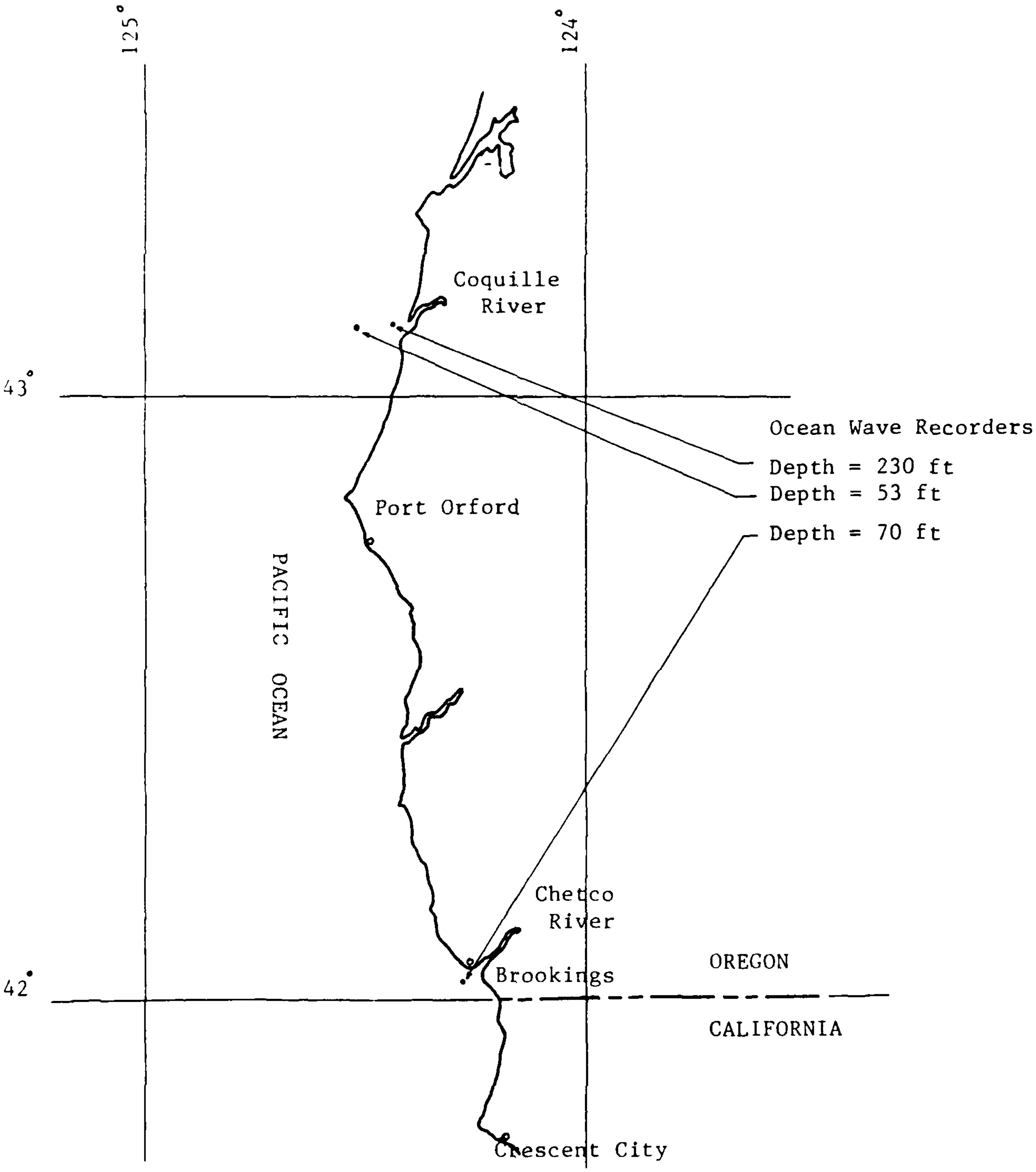

Figure 1. Measurement site locations

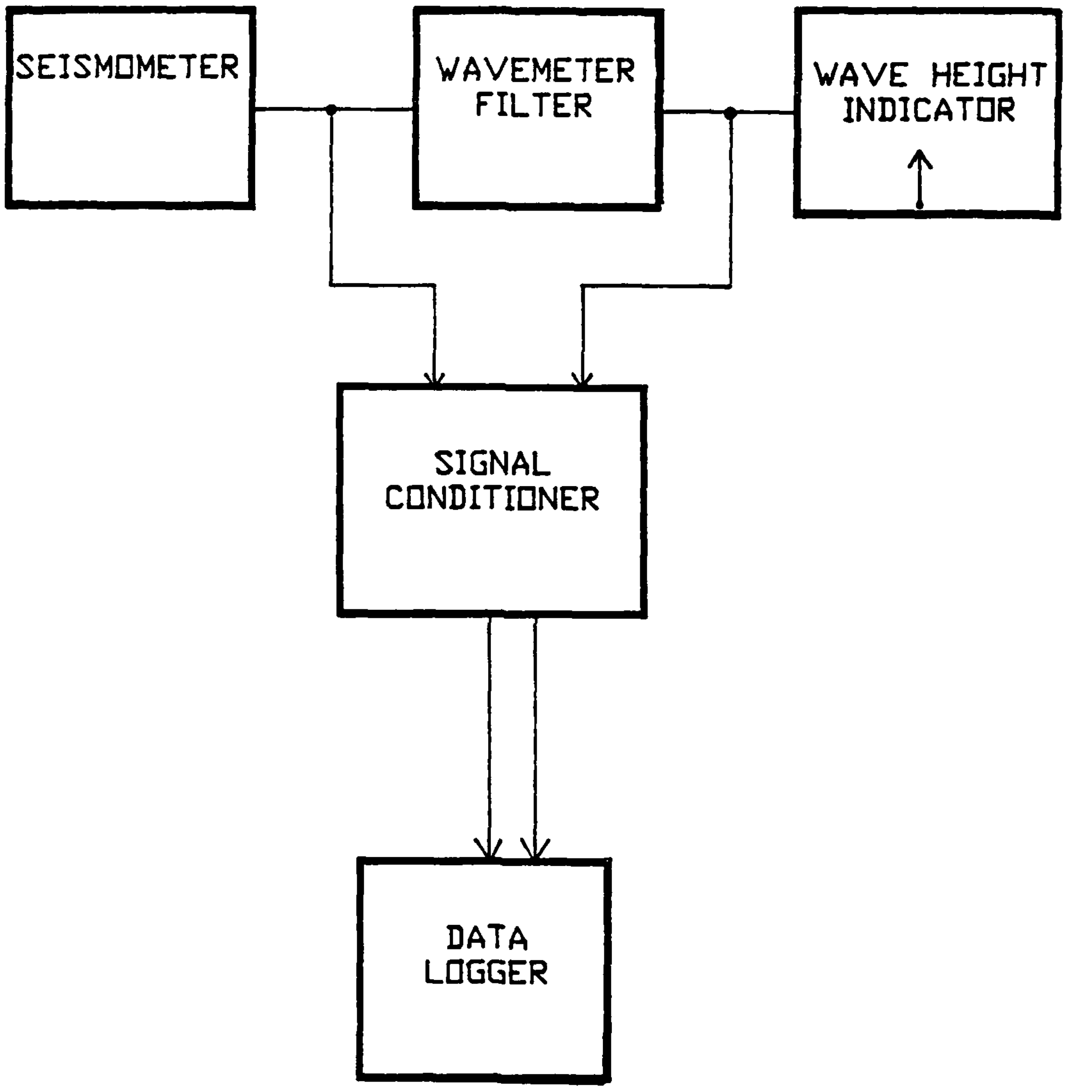

Figure 2. Seismometer data acquisition block diagram

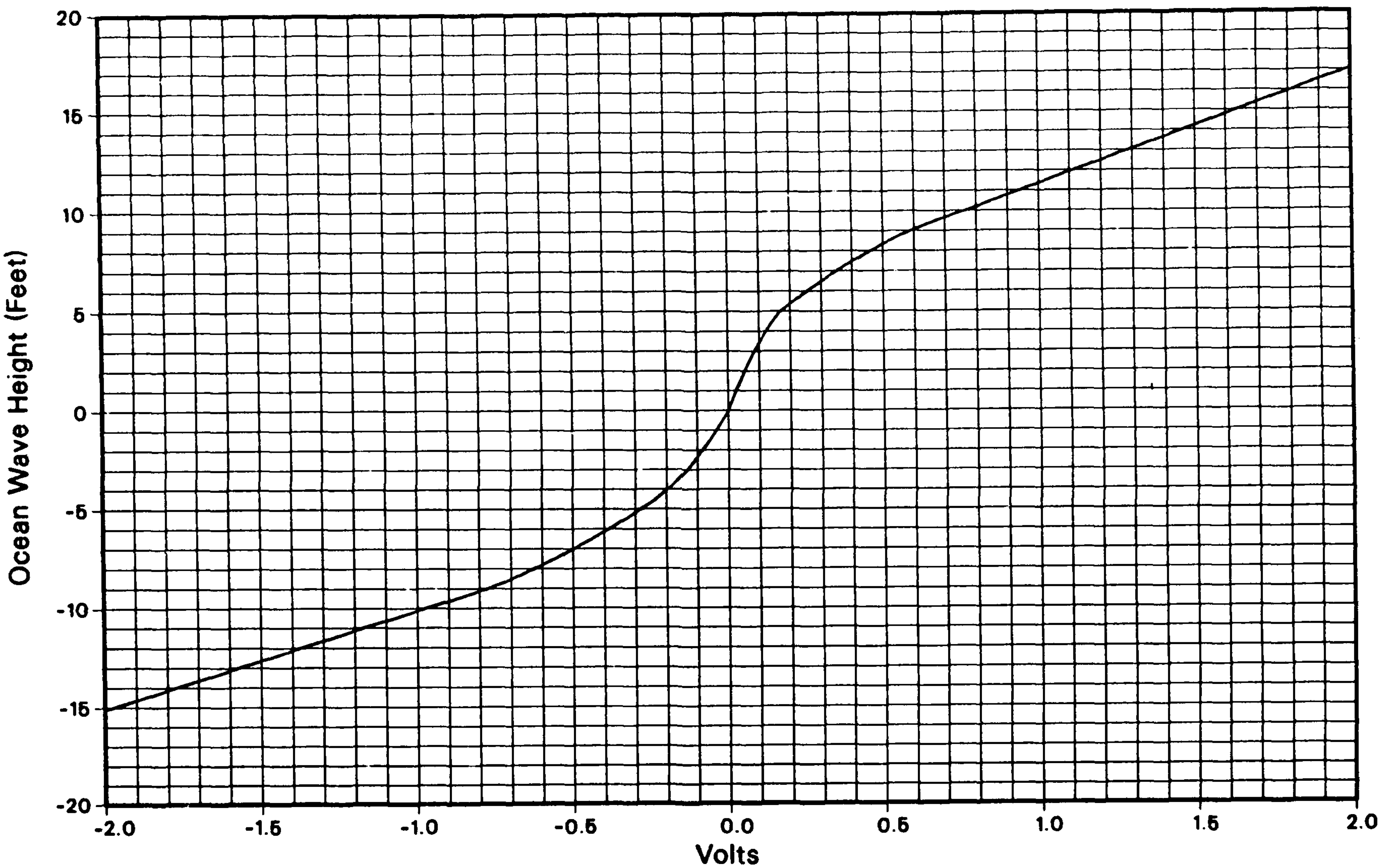

Figure 3. Calibration curve for seismic data from data logger voltage to wave height

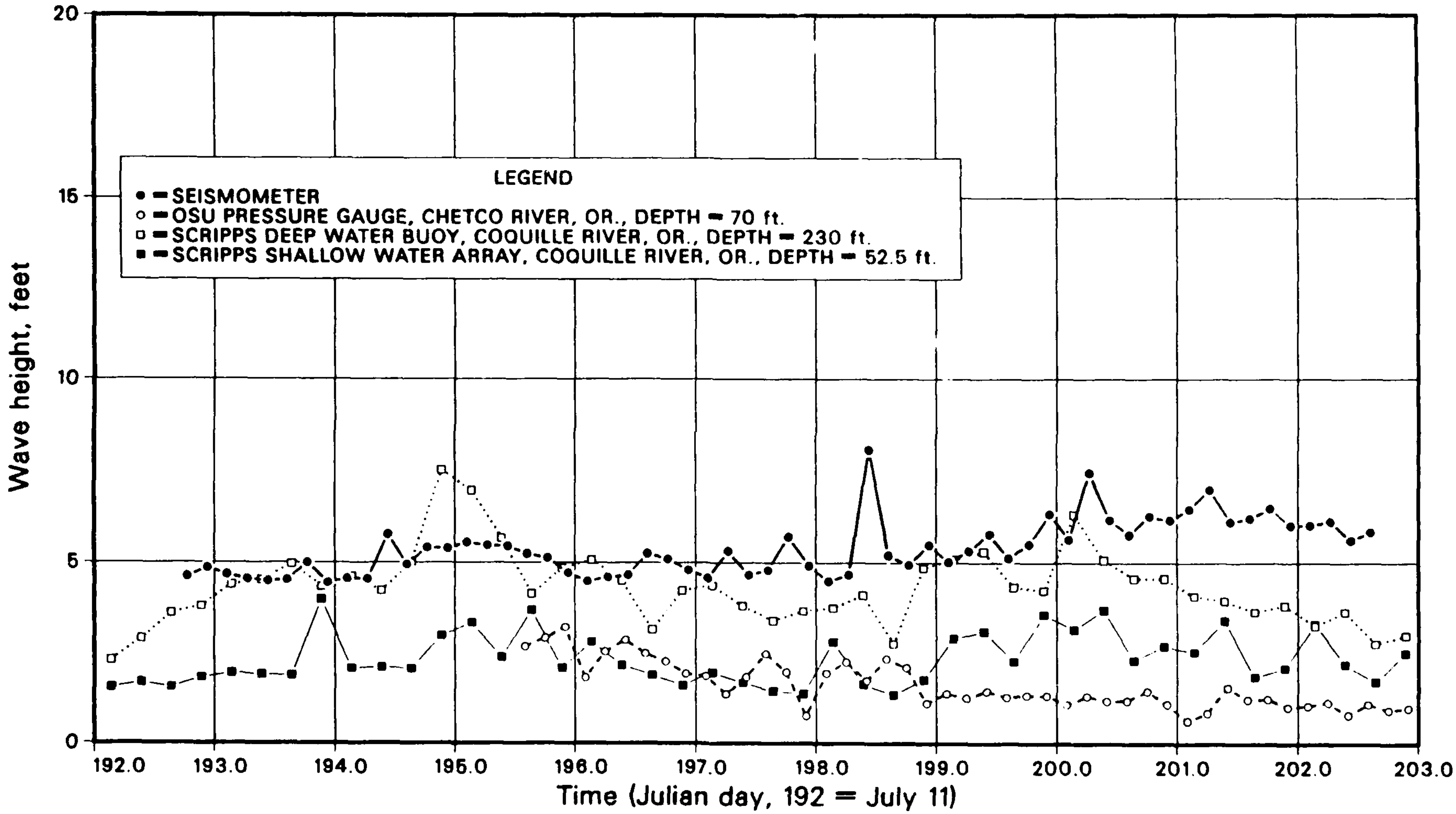

Figure 4. Time series of significant wave heights from 11-21 July 1985

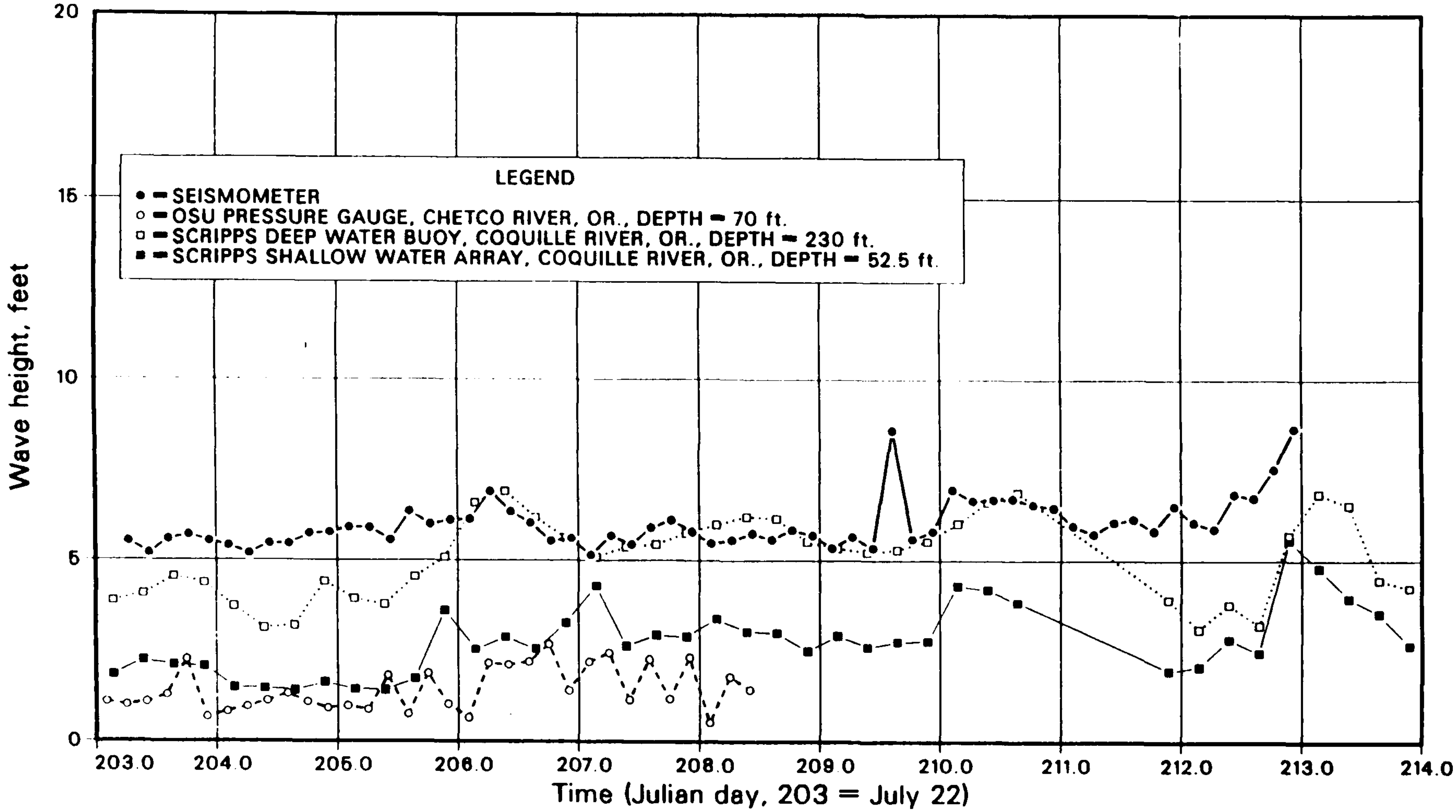

Figure 5. Time series of significant wave heights from 23 July to I August 1985

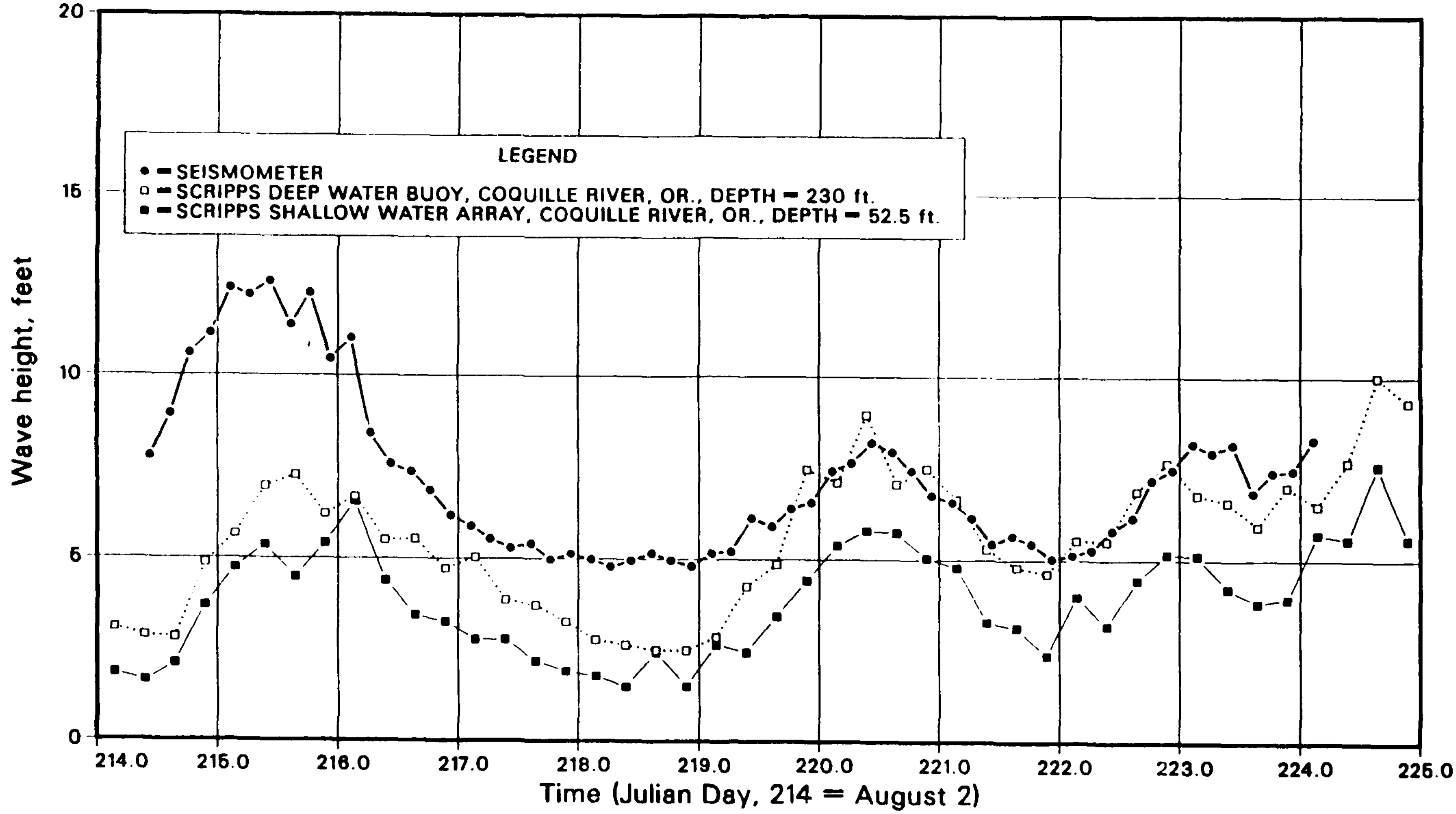

Figure 6. Time series of significant wave heights from 2-12 August 1985

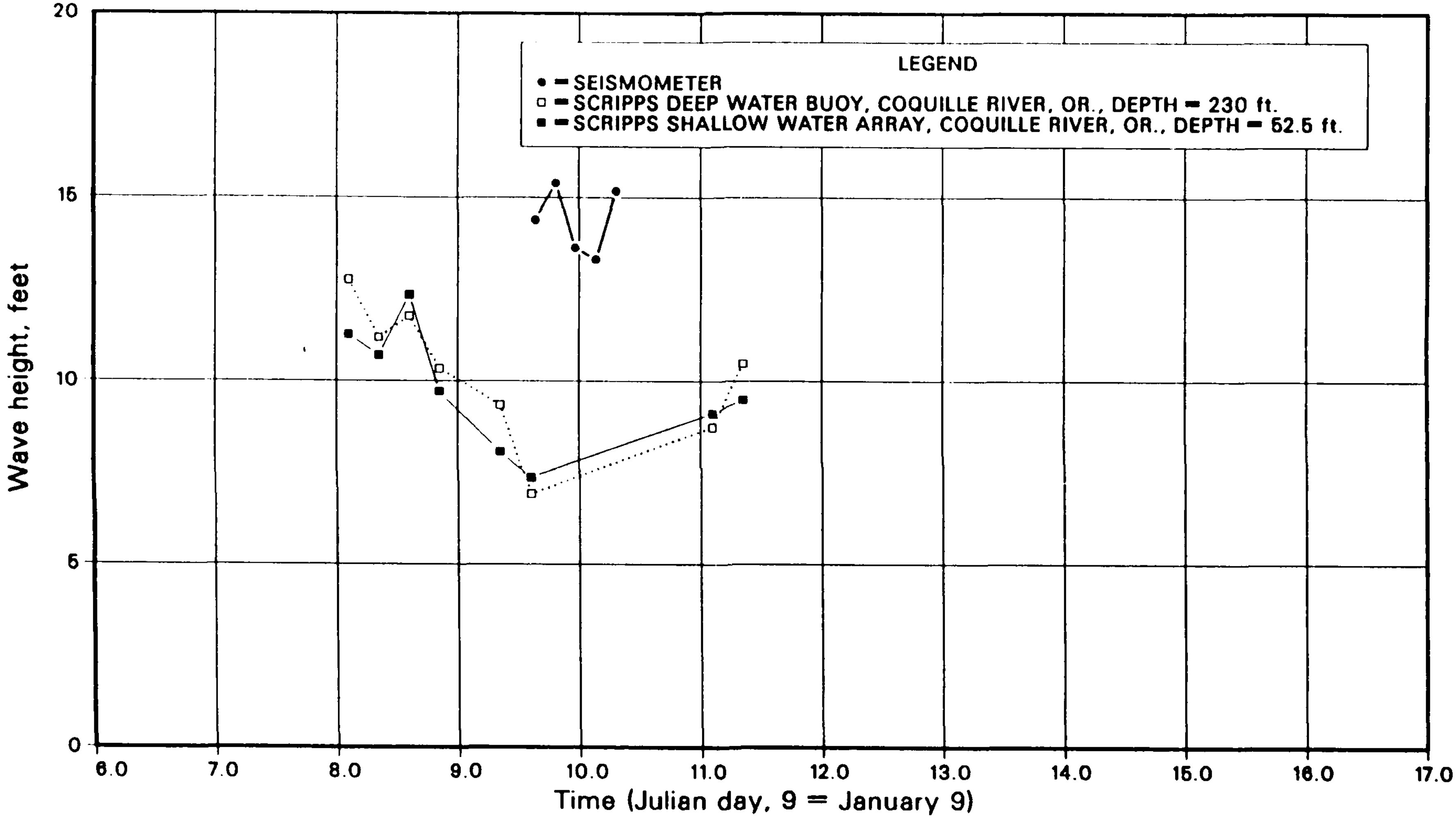

Figure 7. Time series of significant wave heights from 9-10 January 1986

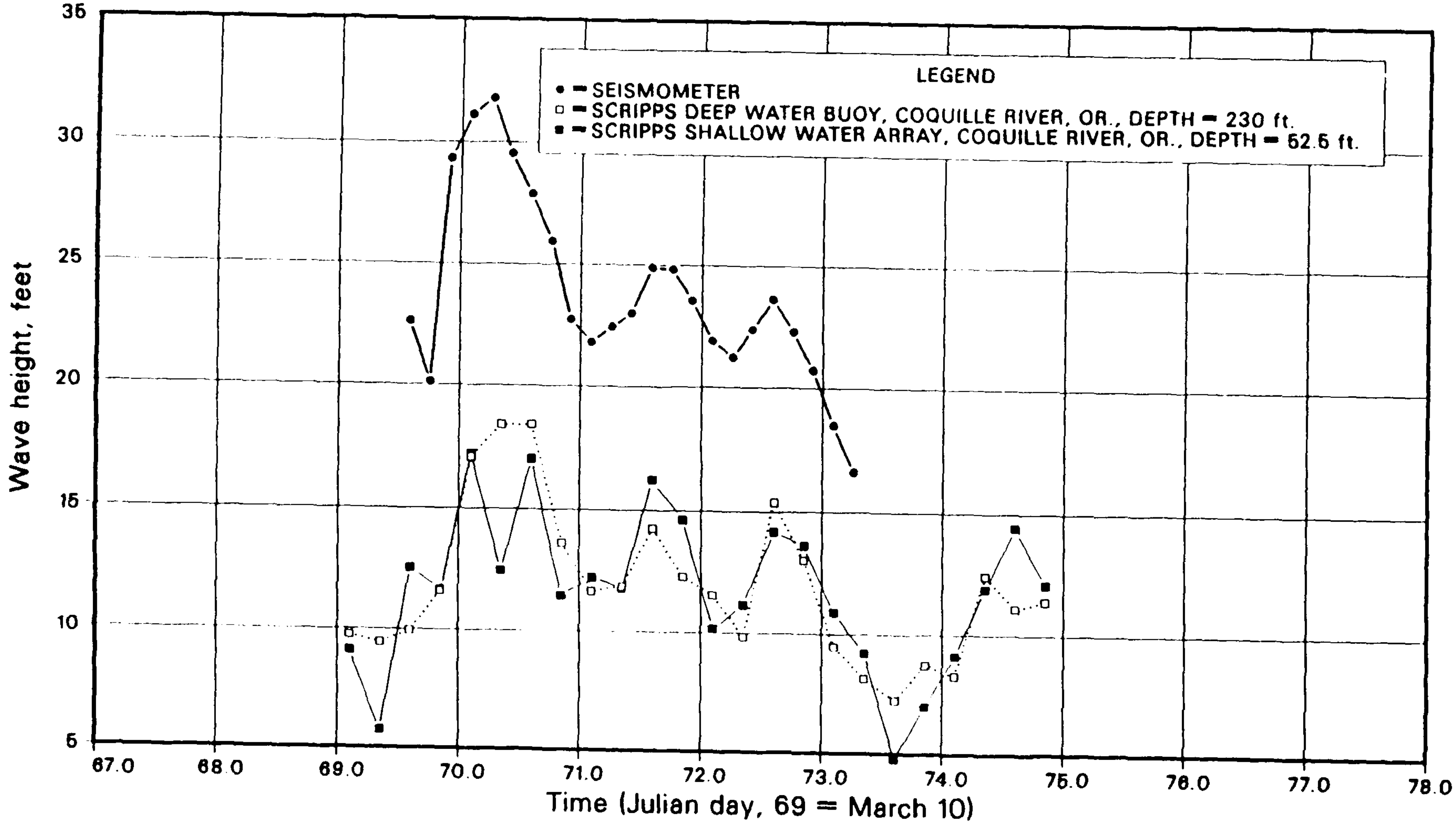

Figure 8. Time series of significant wave heights from 10-14 March 1986

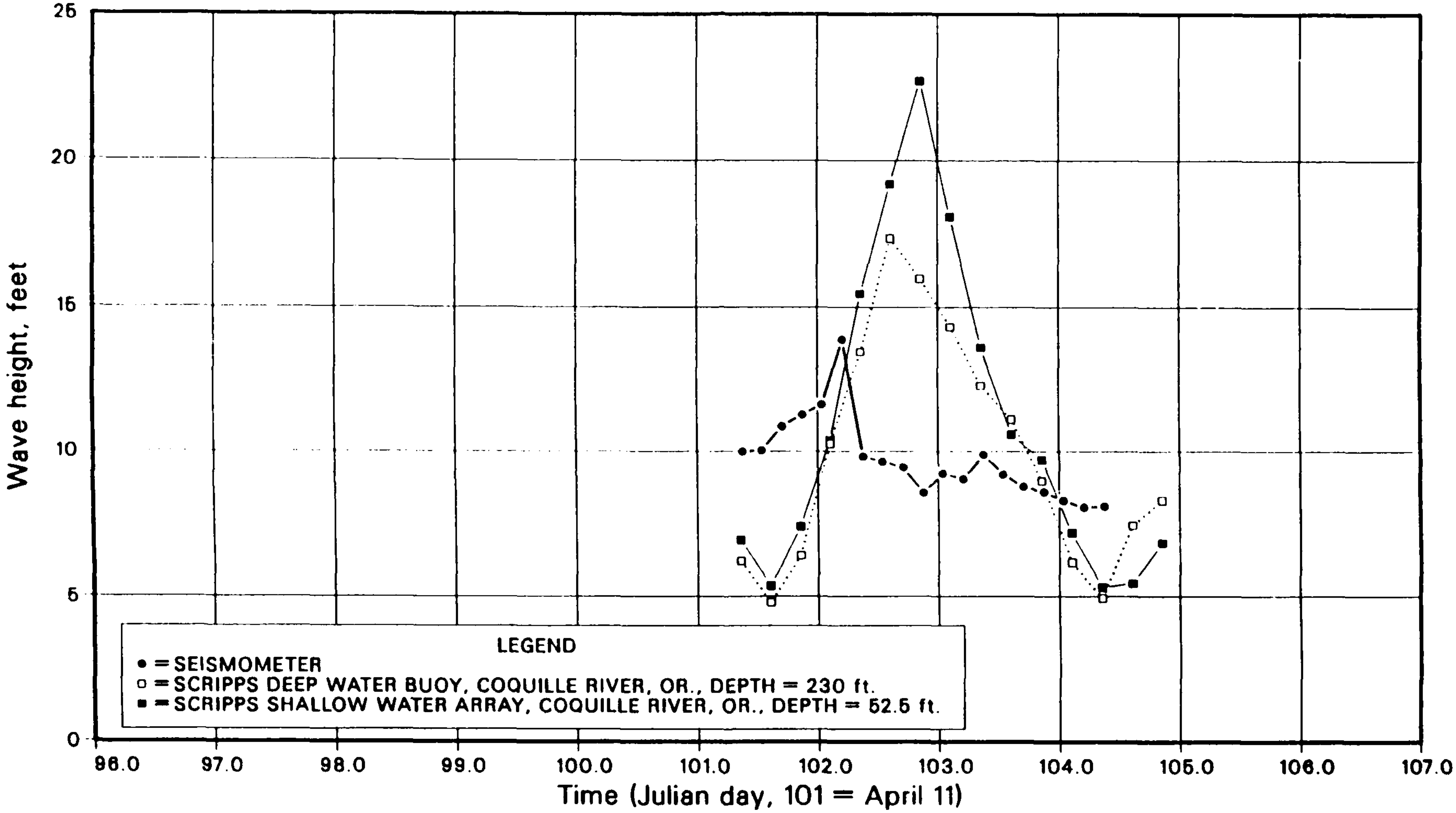

Figure 9. Time series of significant wave heights from 11-14 April 1986

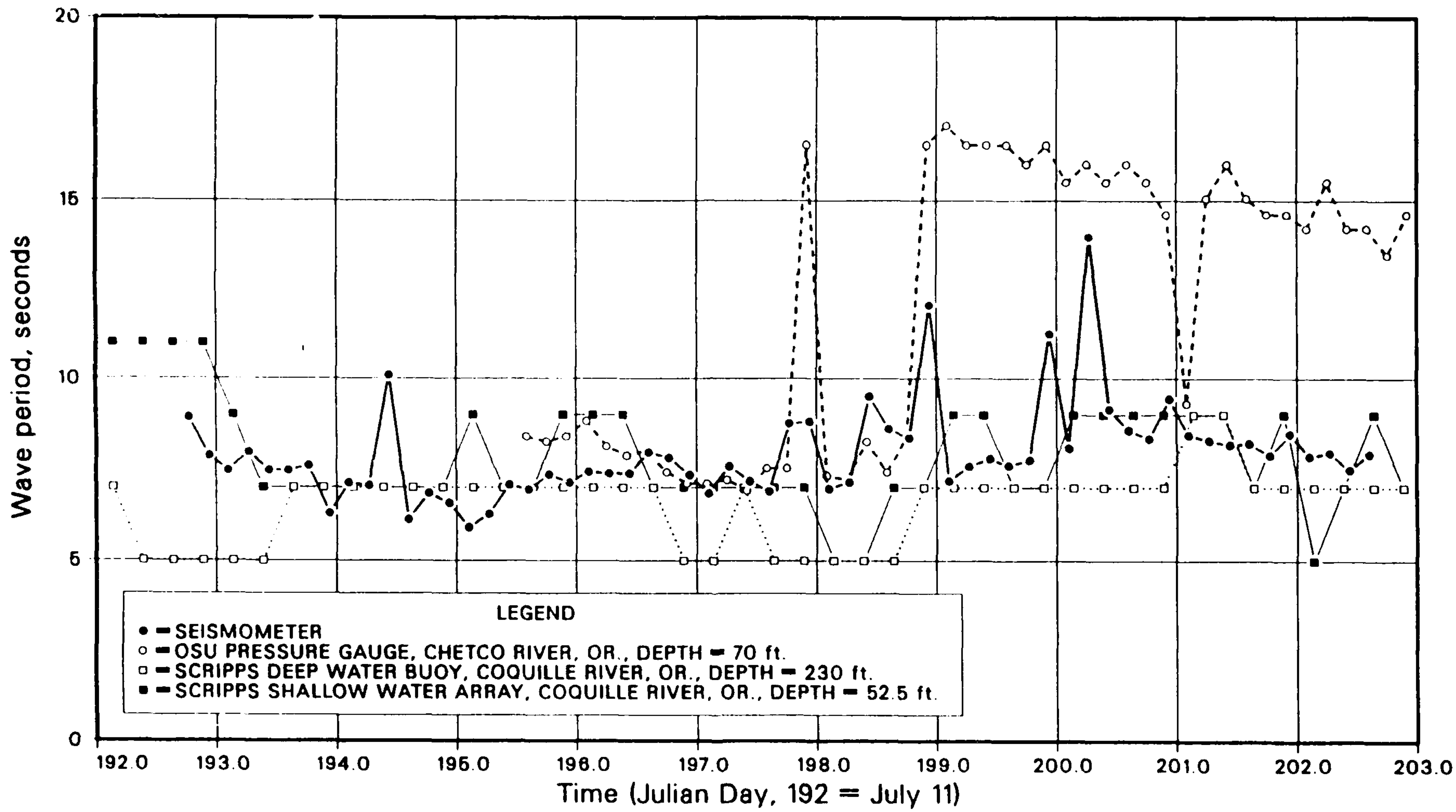

Figure 10. Time series of significant wave periods from 11-21 July 1985

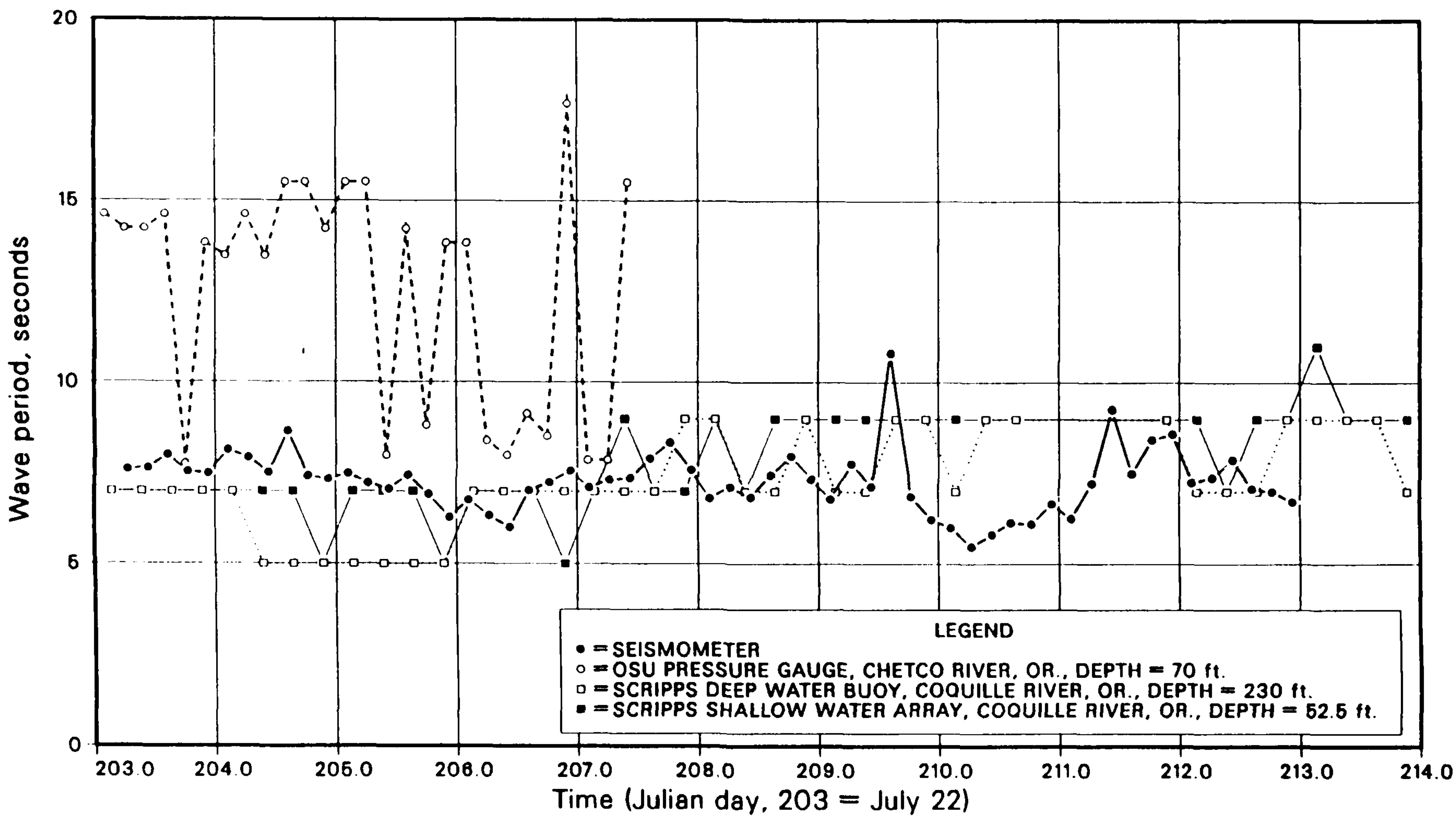

Figure 11. Time series of significant wave periods from 22 July to 1 August 1985

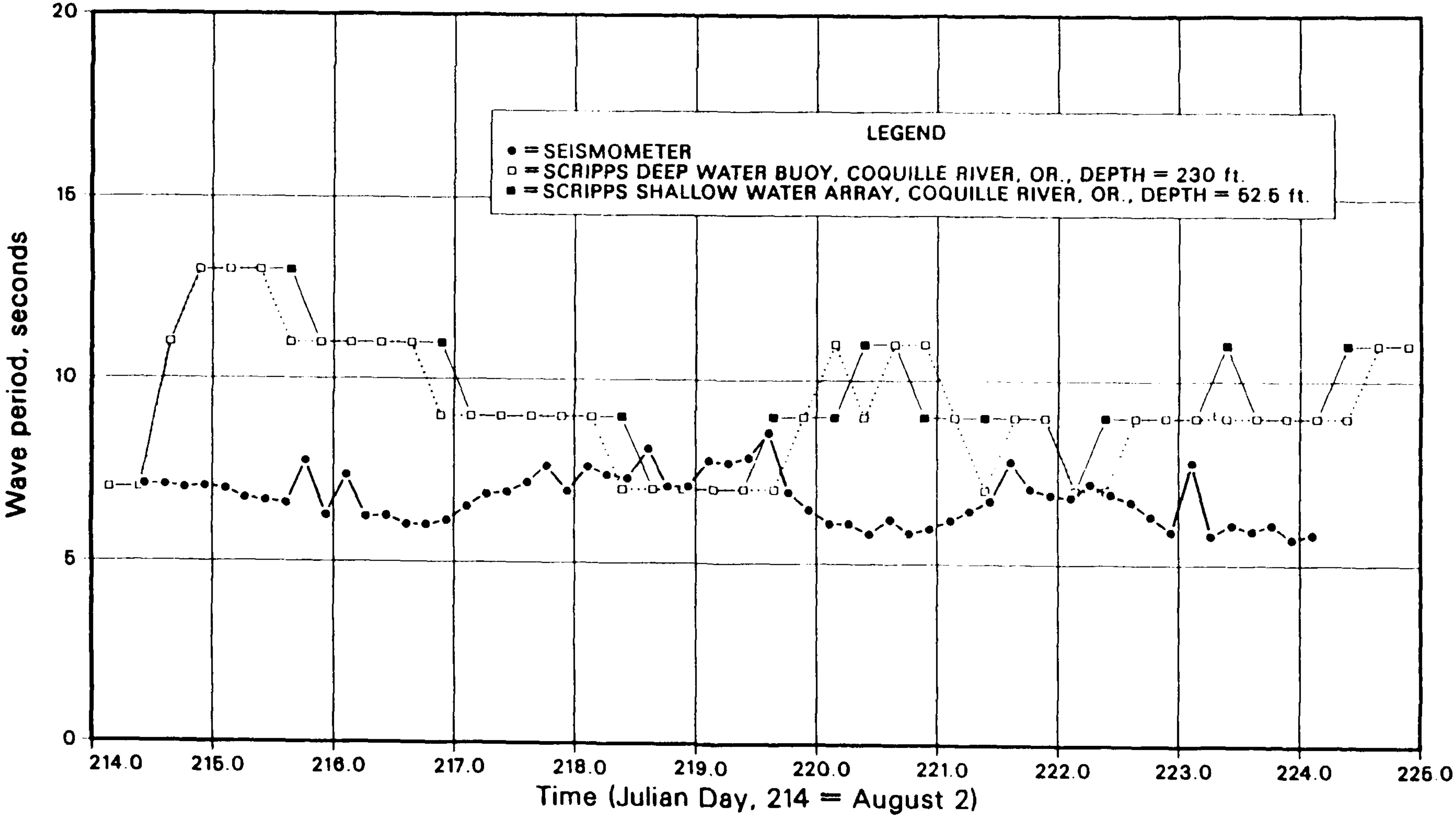

Figure 12. Time series of significant wave periods from 2-12 August 1985

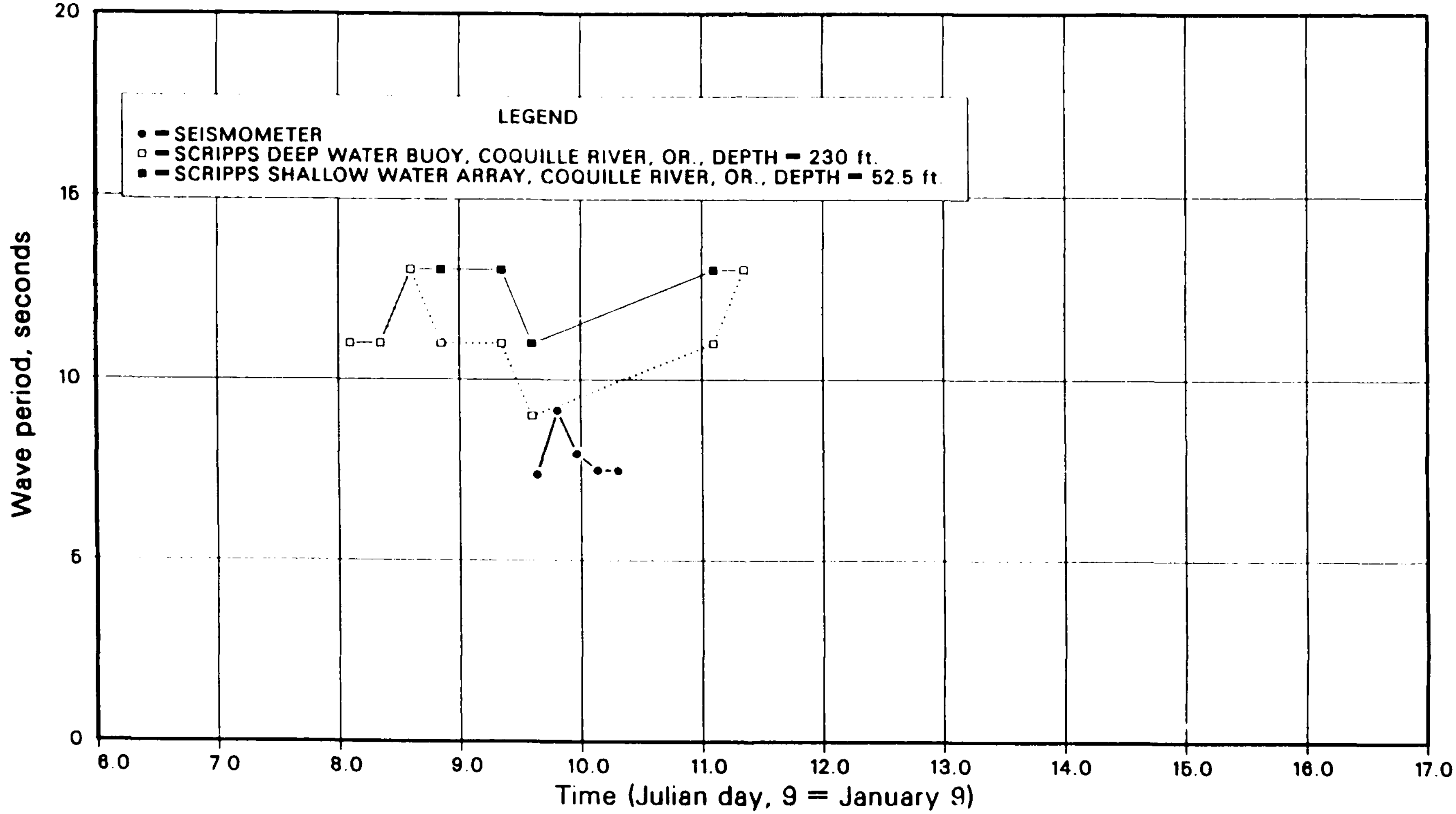

Figure 13. Time series of significant wave periods from 9-10 January 1986

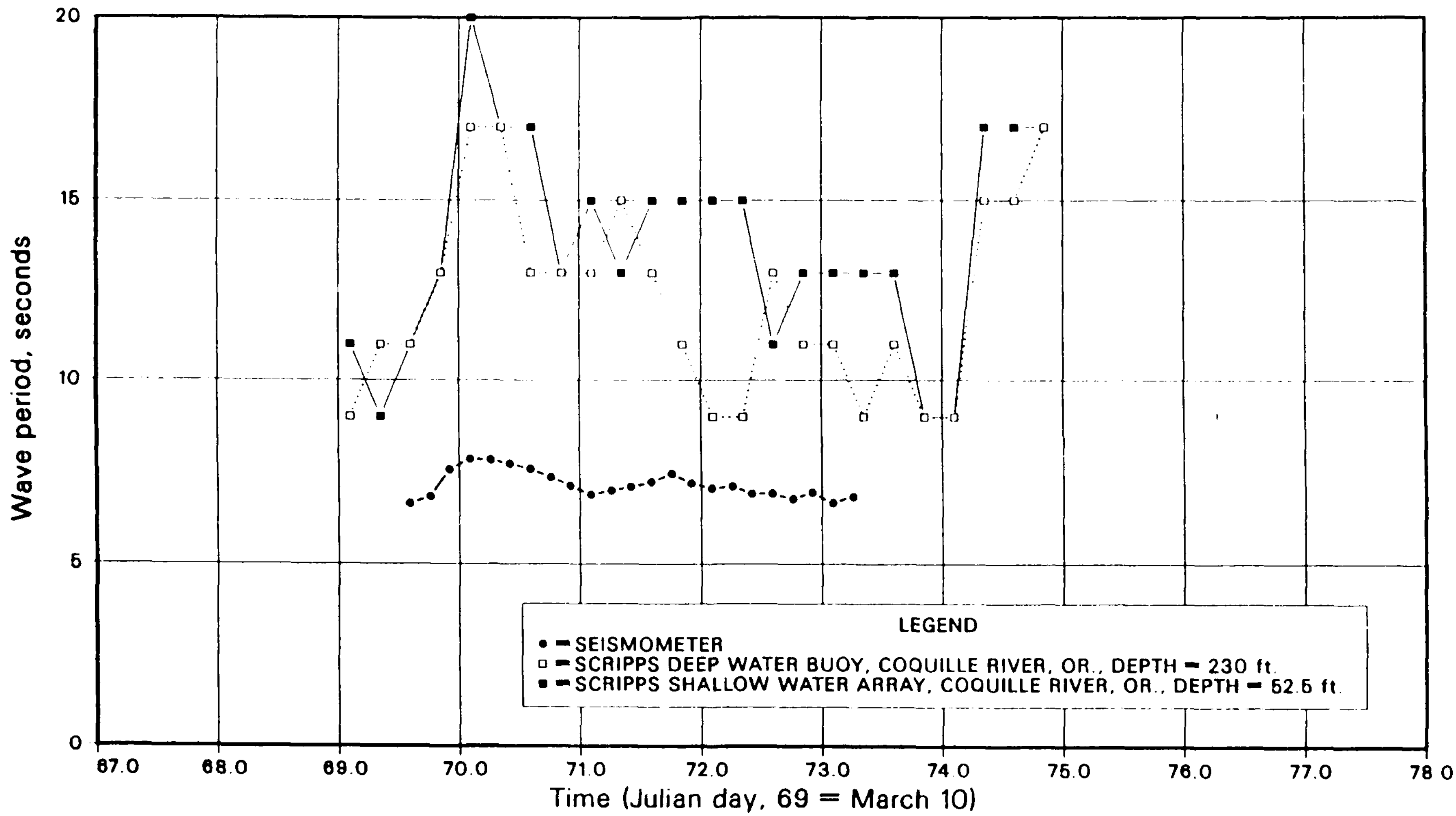

Figure 14. Time series of significant wave periods from 10-14 March 1986

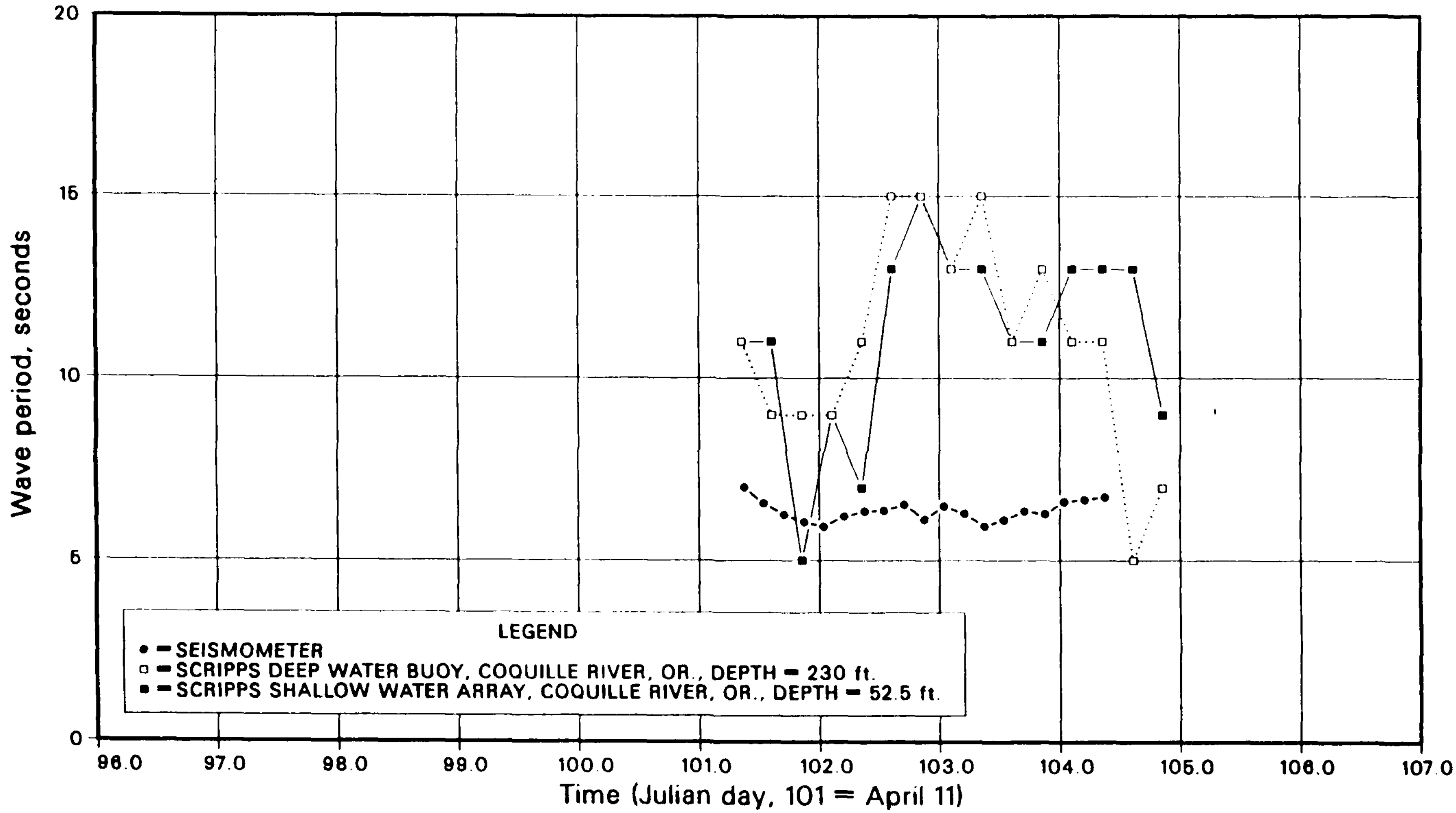

Figure 15. Time series of significant wave periods from 11-14 April 1986

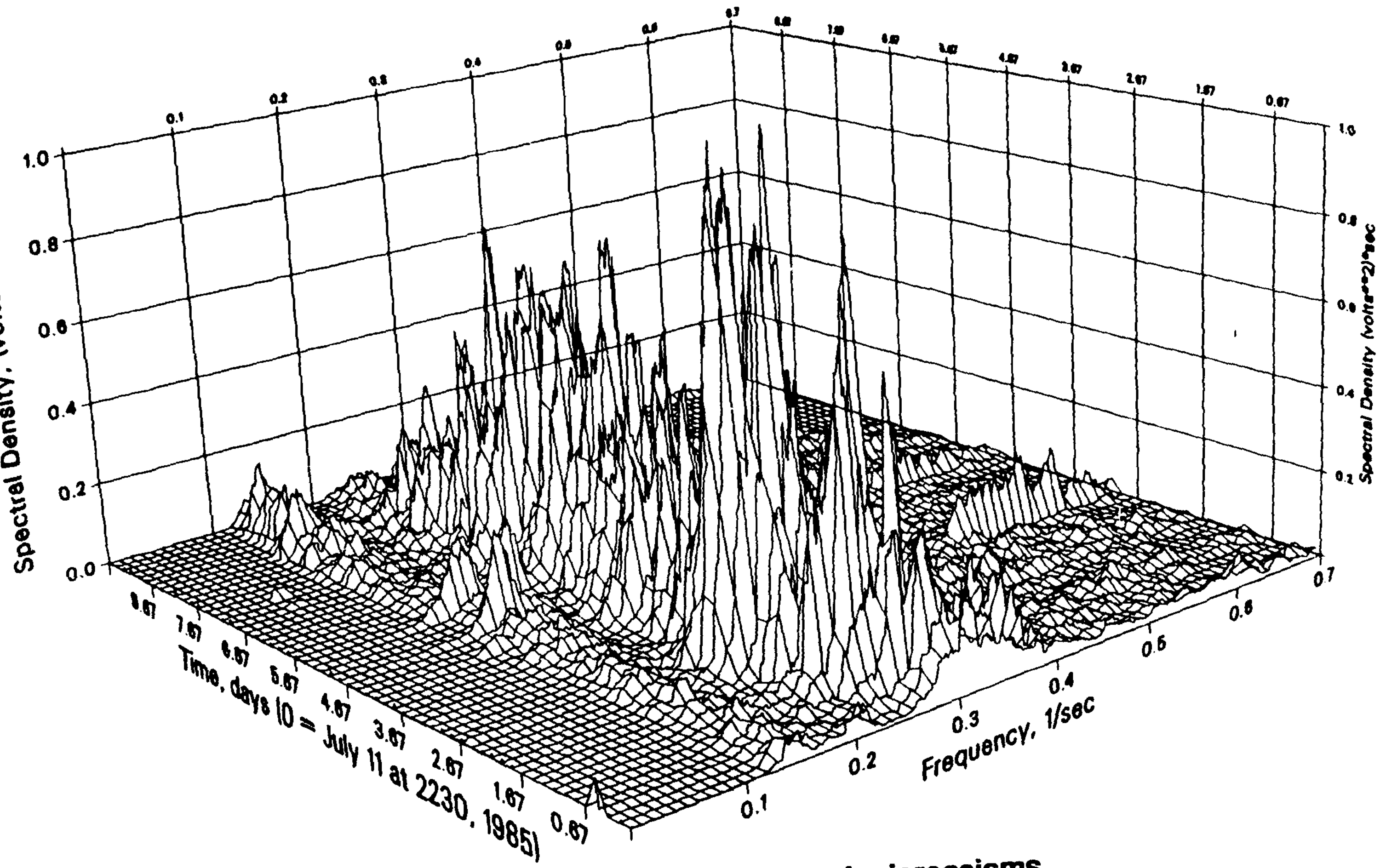

Figure 16. Frequency spectra of microseisms from 11-21 July 1985

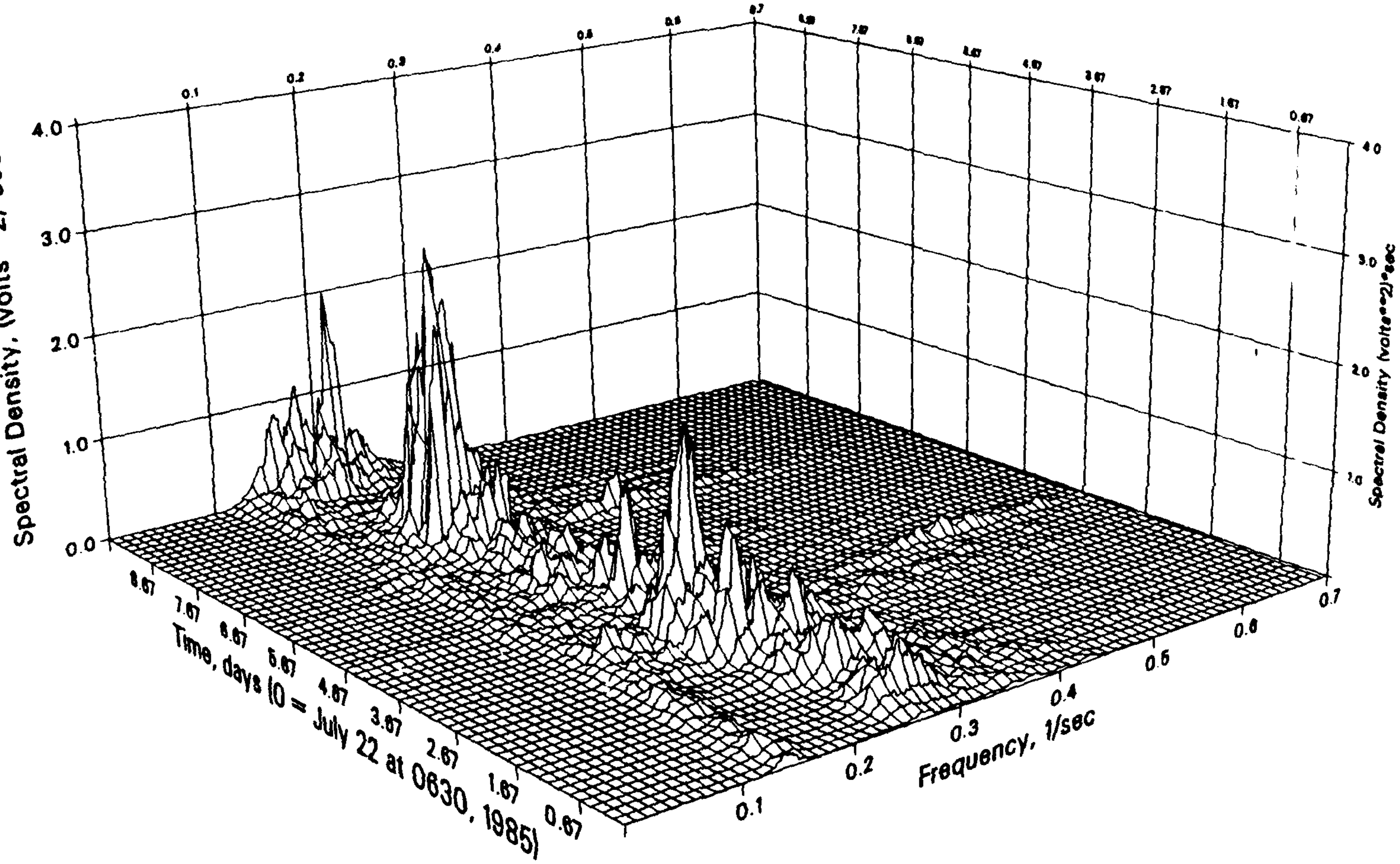

Figure 17. Frequency spectra of microseisms from 22-31 July 1985

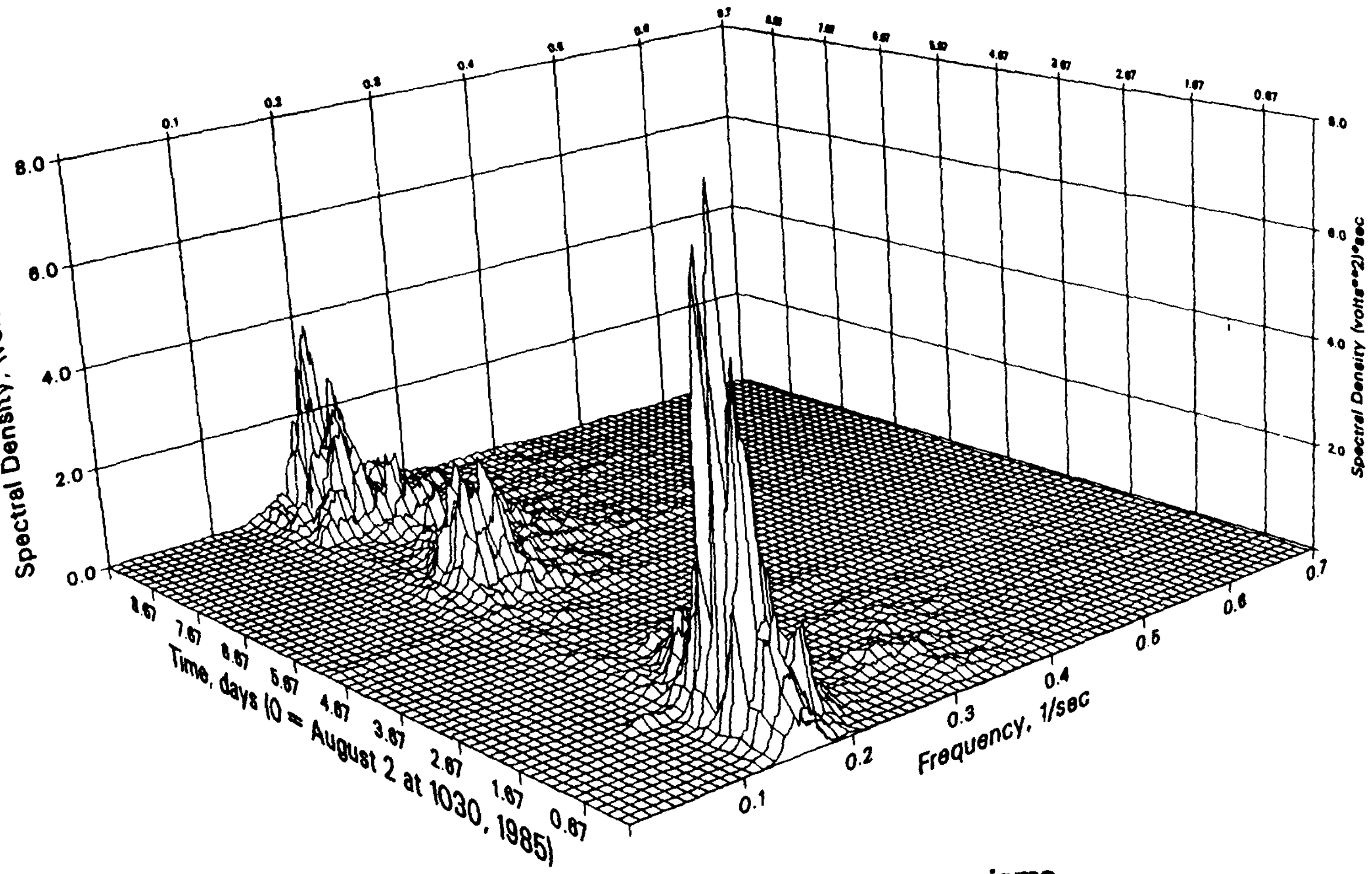

Figure 18. Frequency spectra of microseisms from 2-12 August 1985

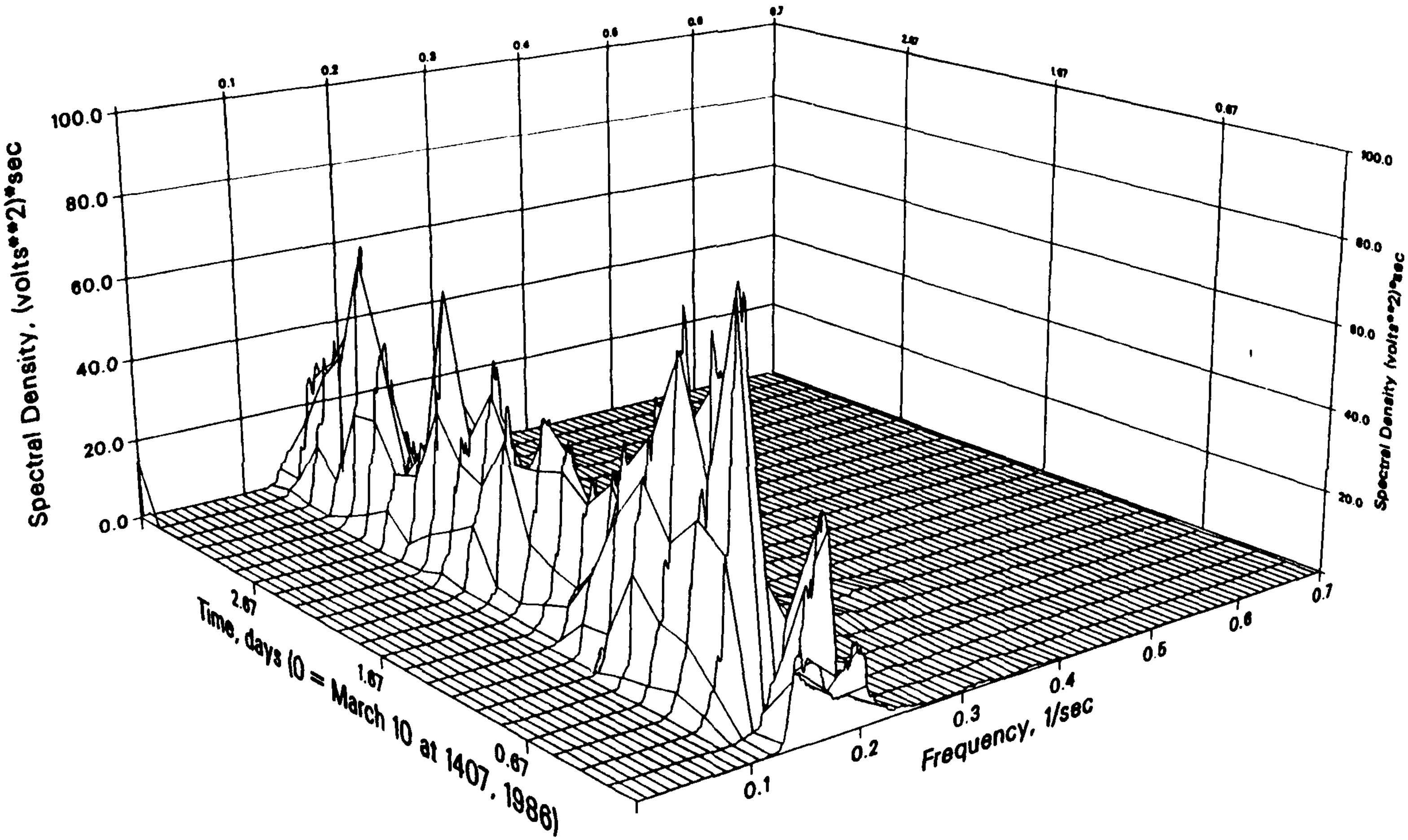

Figure 19. Frequency spectra of microseisms from 10-14 March 1986

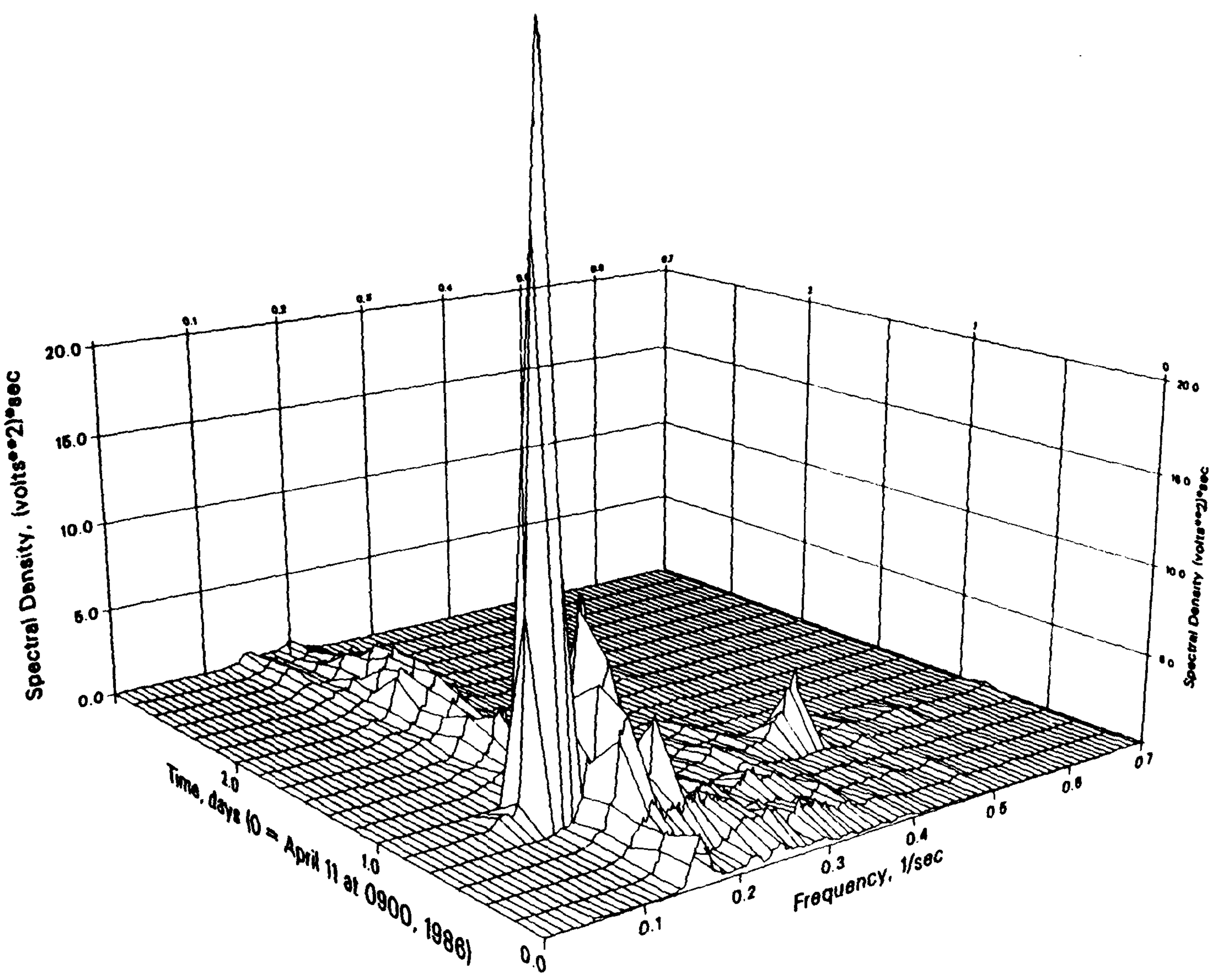

Figure 20. Frequency spectra of microseisms from 11-14 April 1986

(August 2-12, 1985)

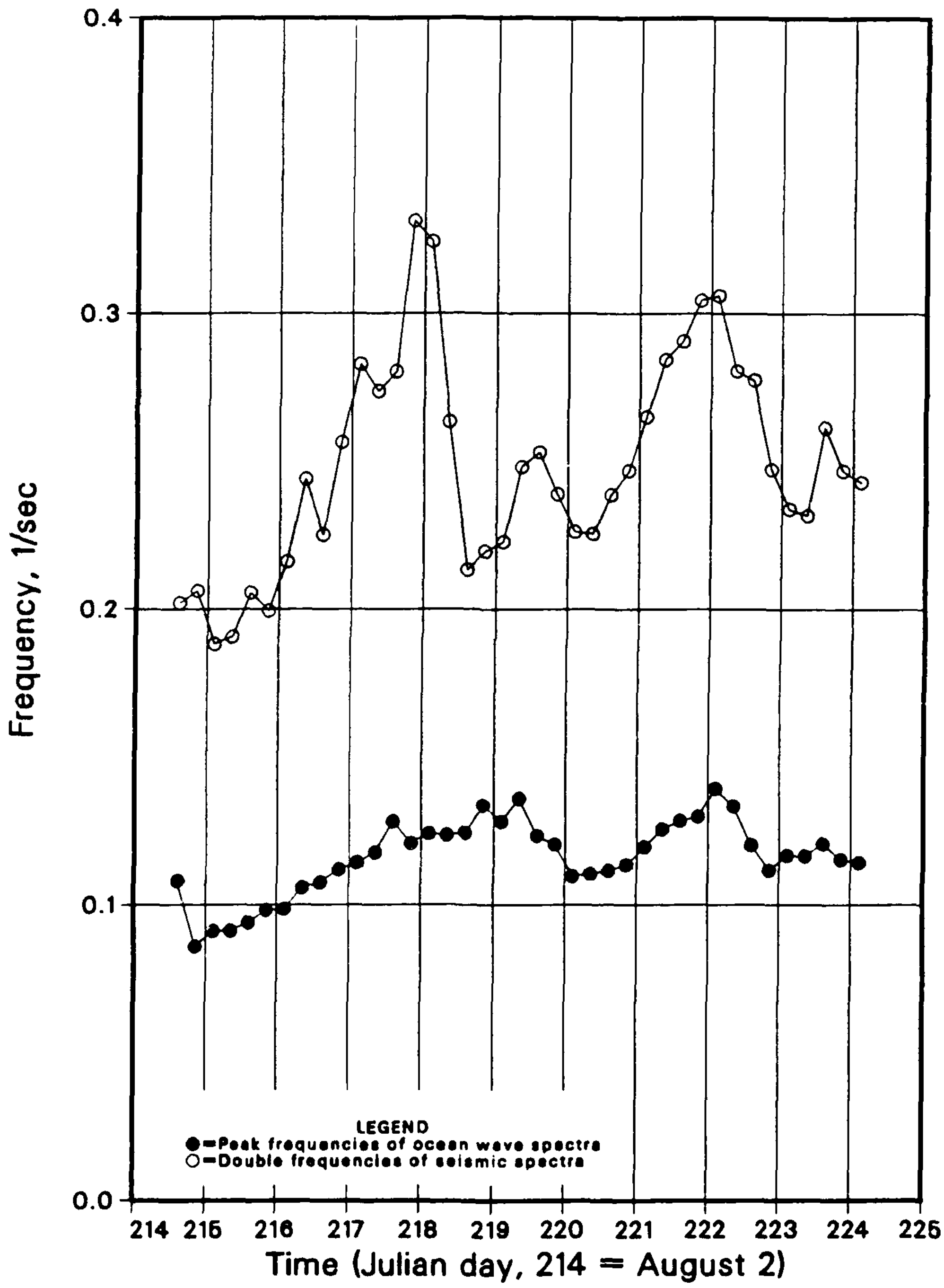

Figure 21. Dispersive change of peak frequency in seismic and ocean wave spectra at water depth of 230 ft

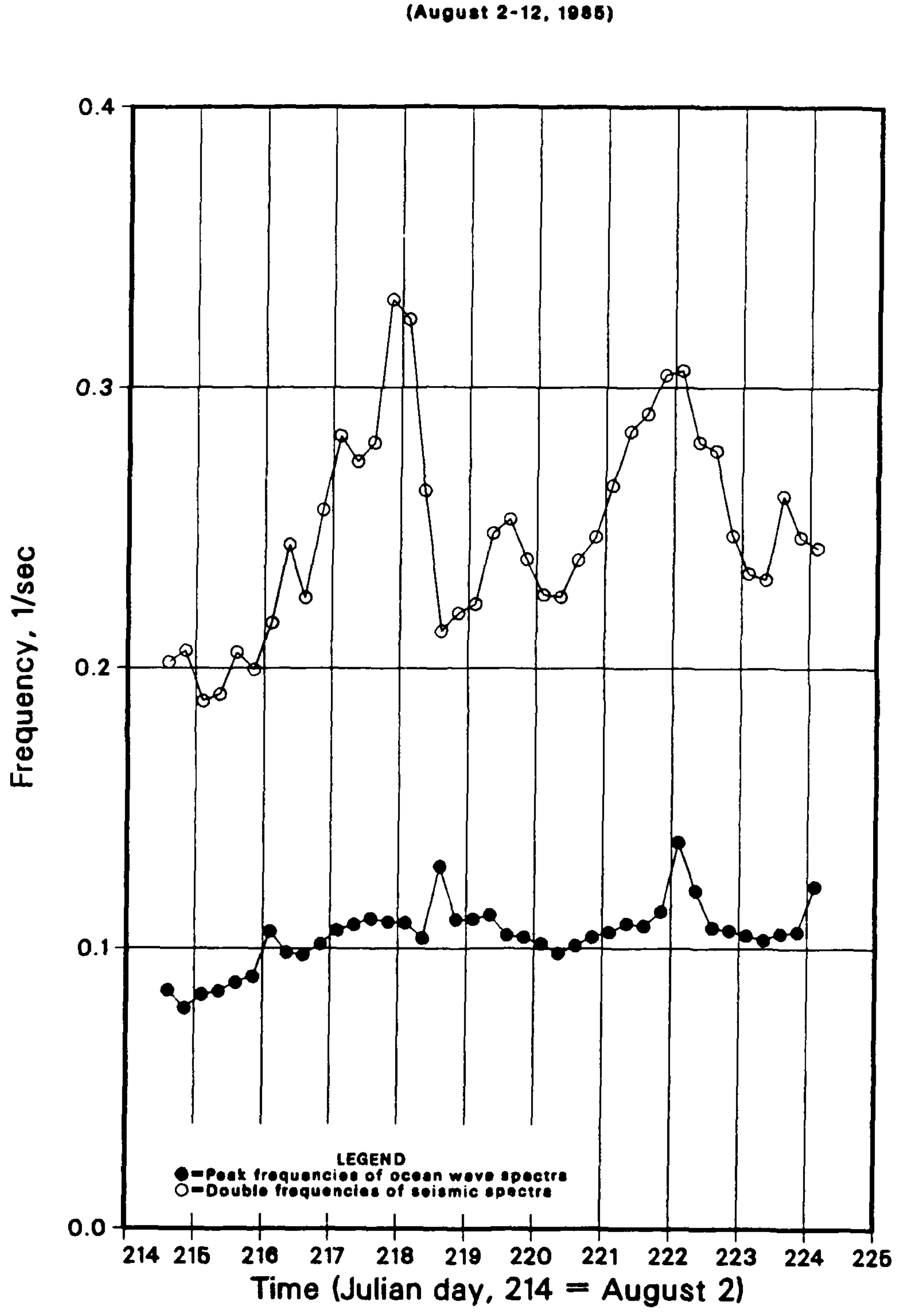

Figure 22. Dispersive change of peak frequency in seismic and ocean wave spectra at water depth of 52 ft

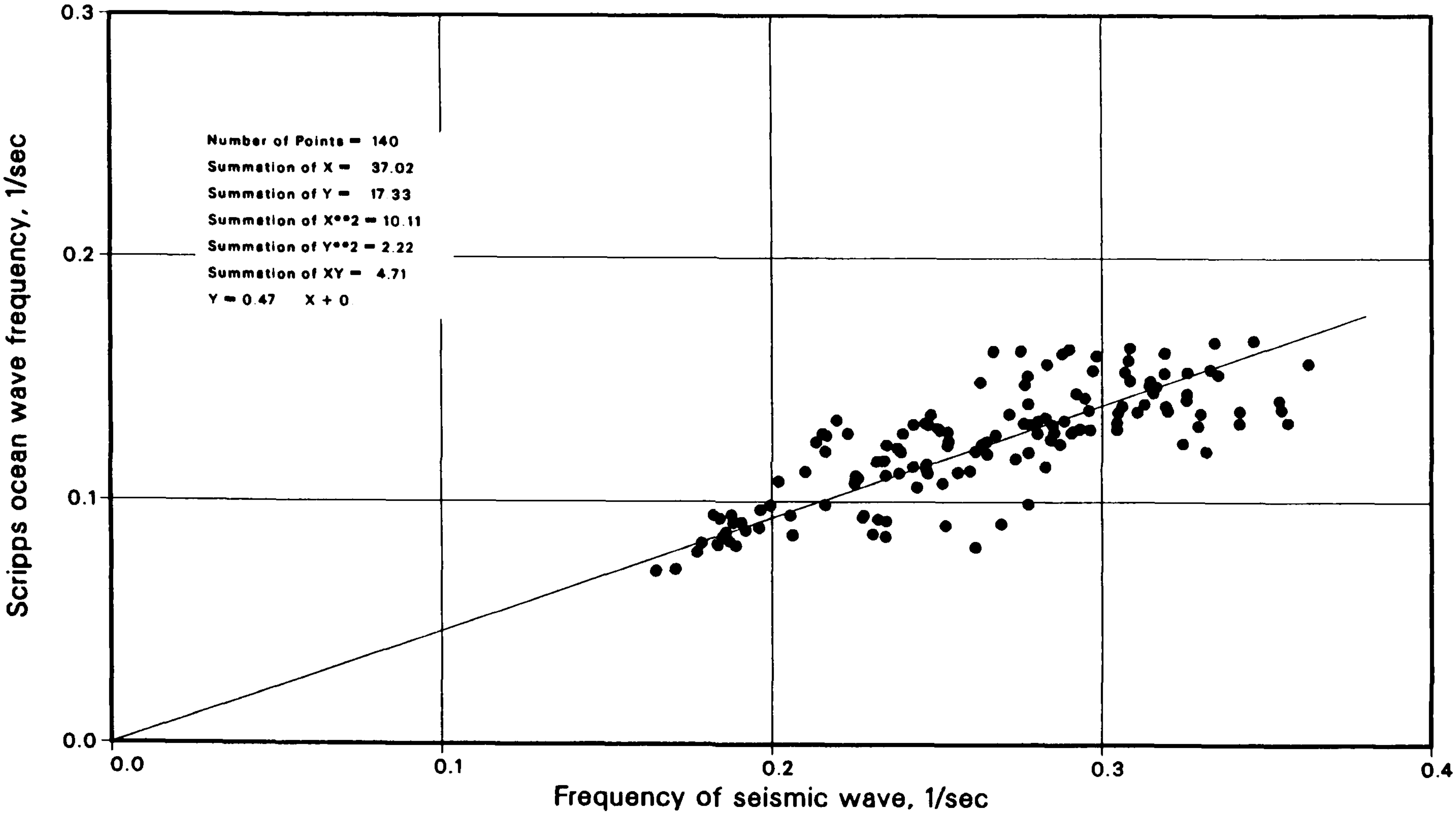

Figure 23. Microseisms frequency versus ocean wave frequency at water depth of 230 ft from July and August 1985 and March and April 1986

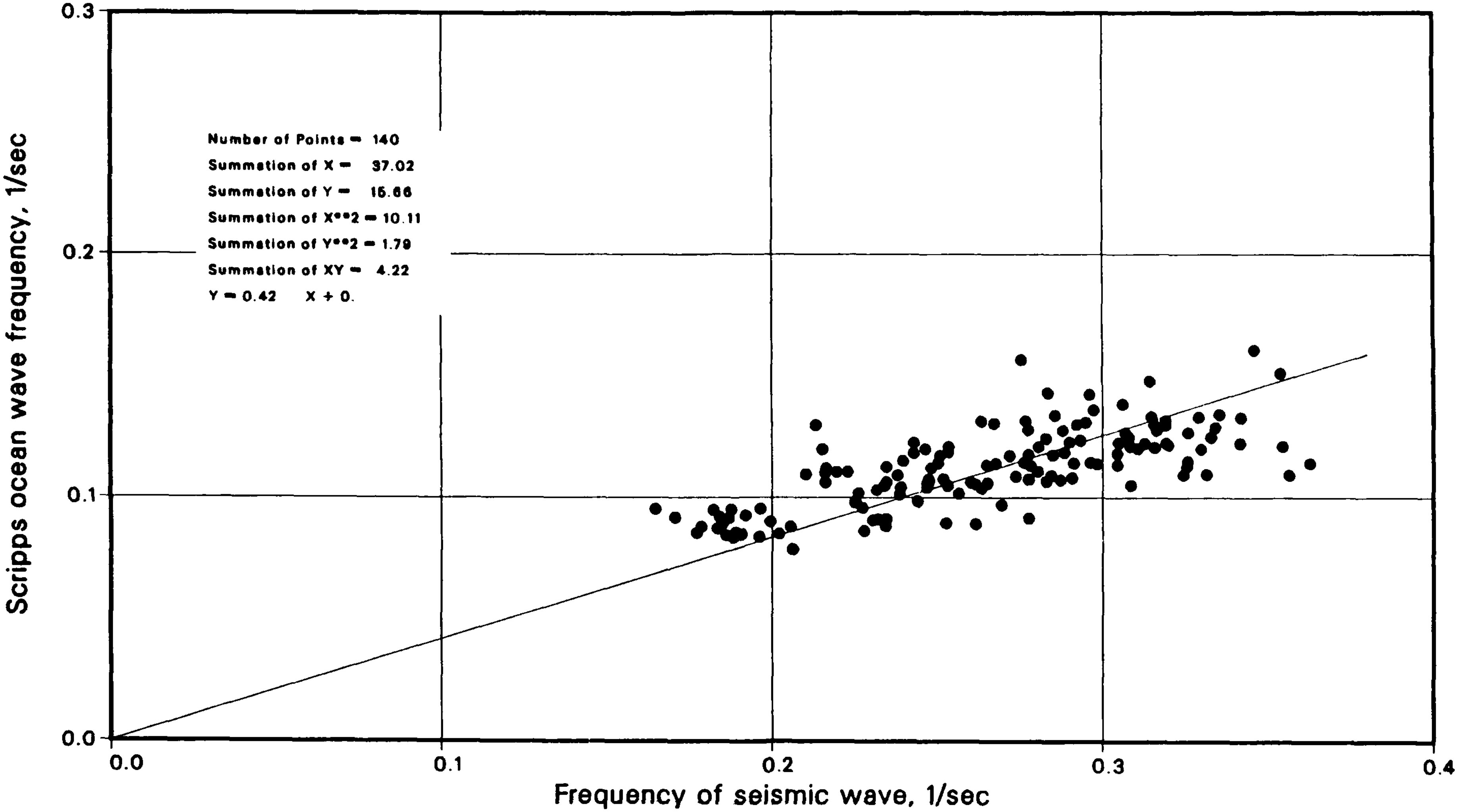

Figure 24. Microseisms frequency versus ocean wave frequency at water depth of 52 ft from July and August 1985 and March and April 1986

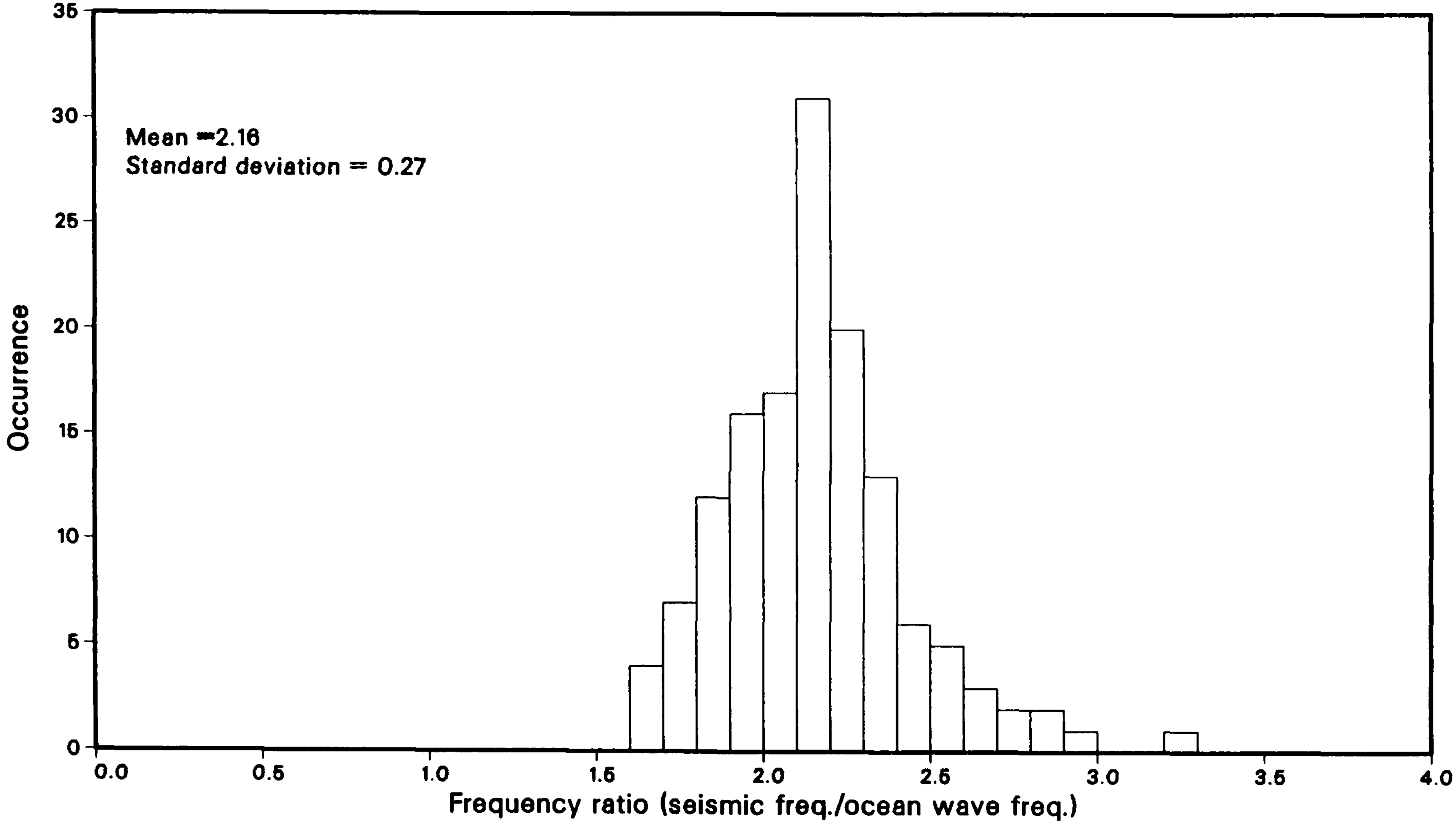

Figure 25. Microseisms frequency versus ocean wave frequency. Ratio of peak spectrum frequencies at water depth of 230 ft from July and August 1985 and March and April 1986

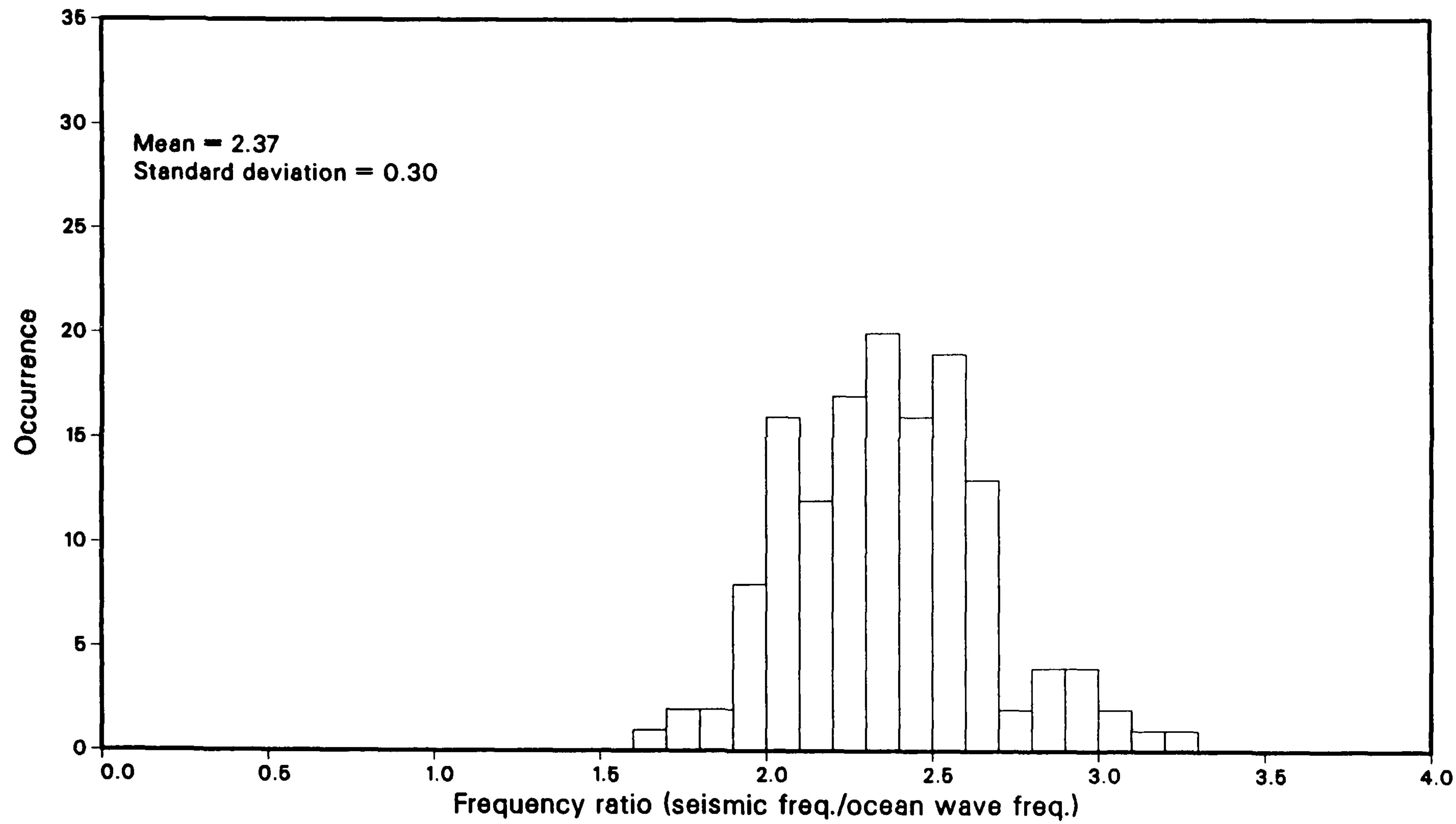

Figure 26. Microseisms frequency versus ocean wave frequency. Ratio of peak spectrum frequencies at water depth of 230 ft from July and August 1985 and March and April 1986

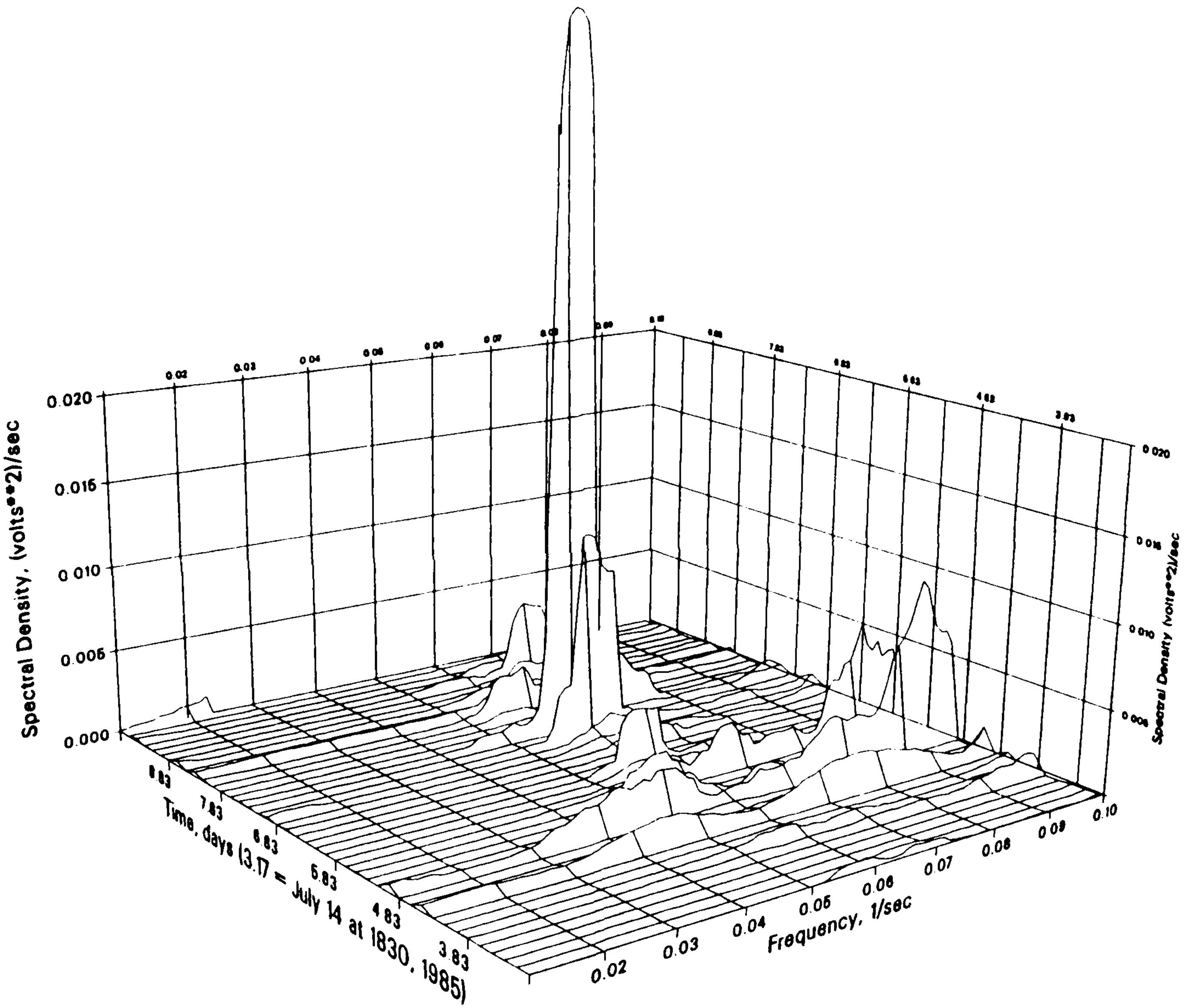

Figure 27. Frequency spectra of microseisms from 14-21 July 1985

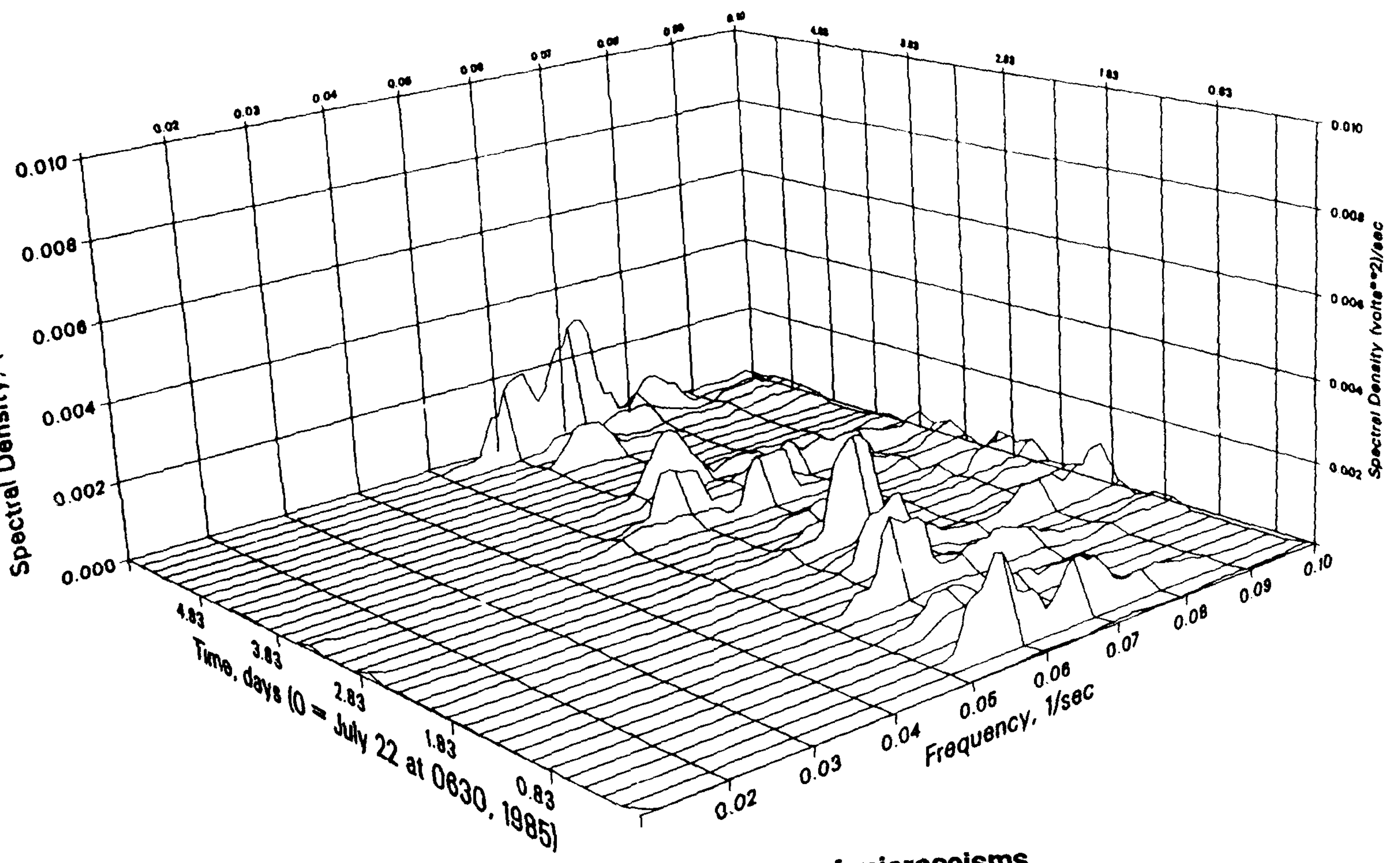

Figure 28. Frequency spectra of microseisms from 22-27 July 1985

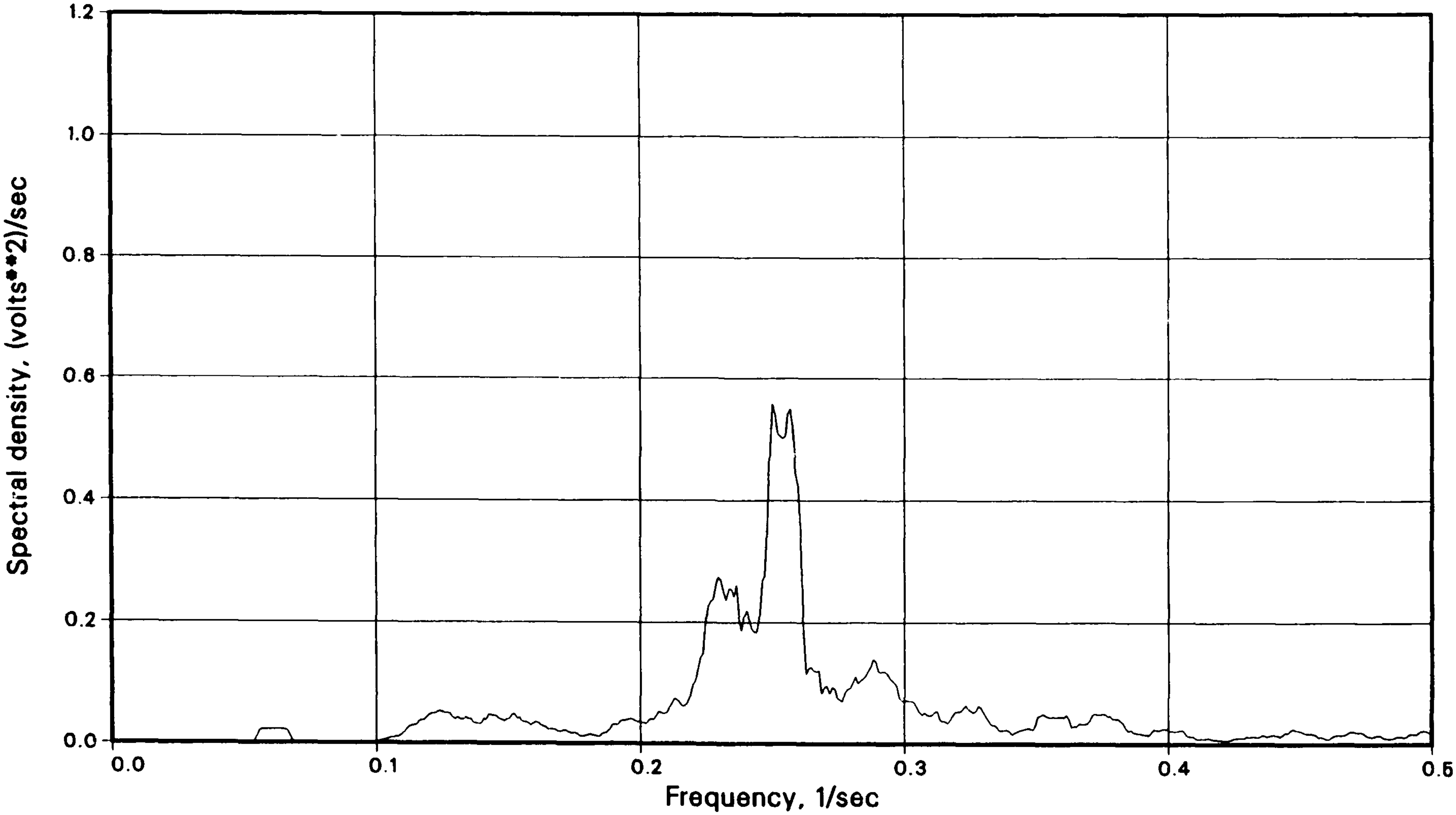

Figure 29. Frequency spectrum of microseisms from 19 July 1985 at 0630

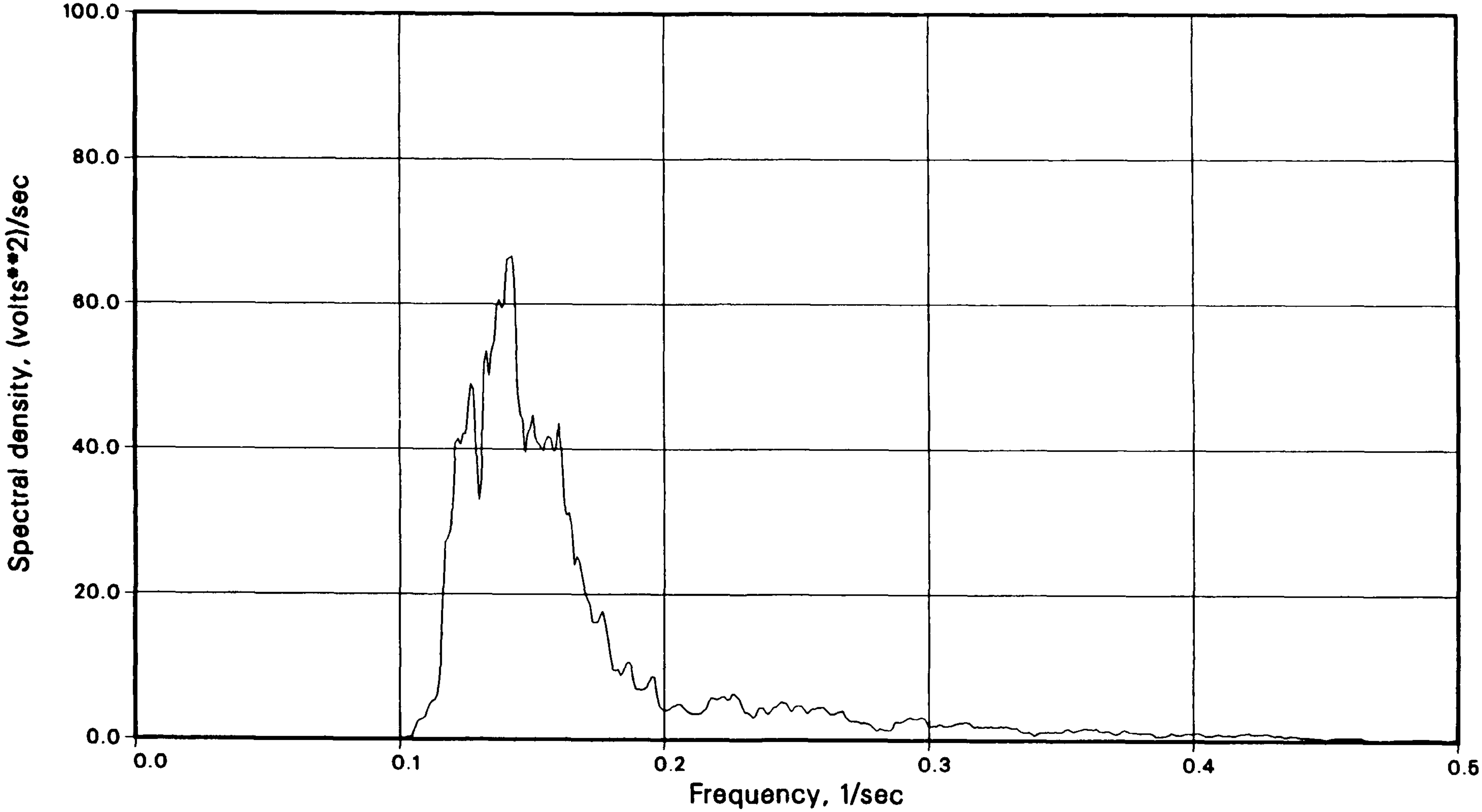

Figure 30. Frequency spectrum of microseisms from 11 March 1986 at 1007

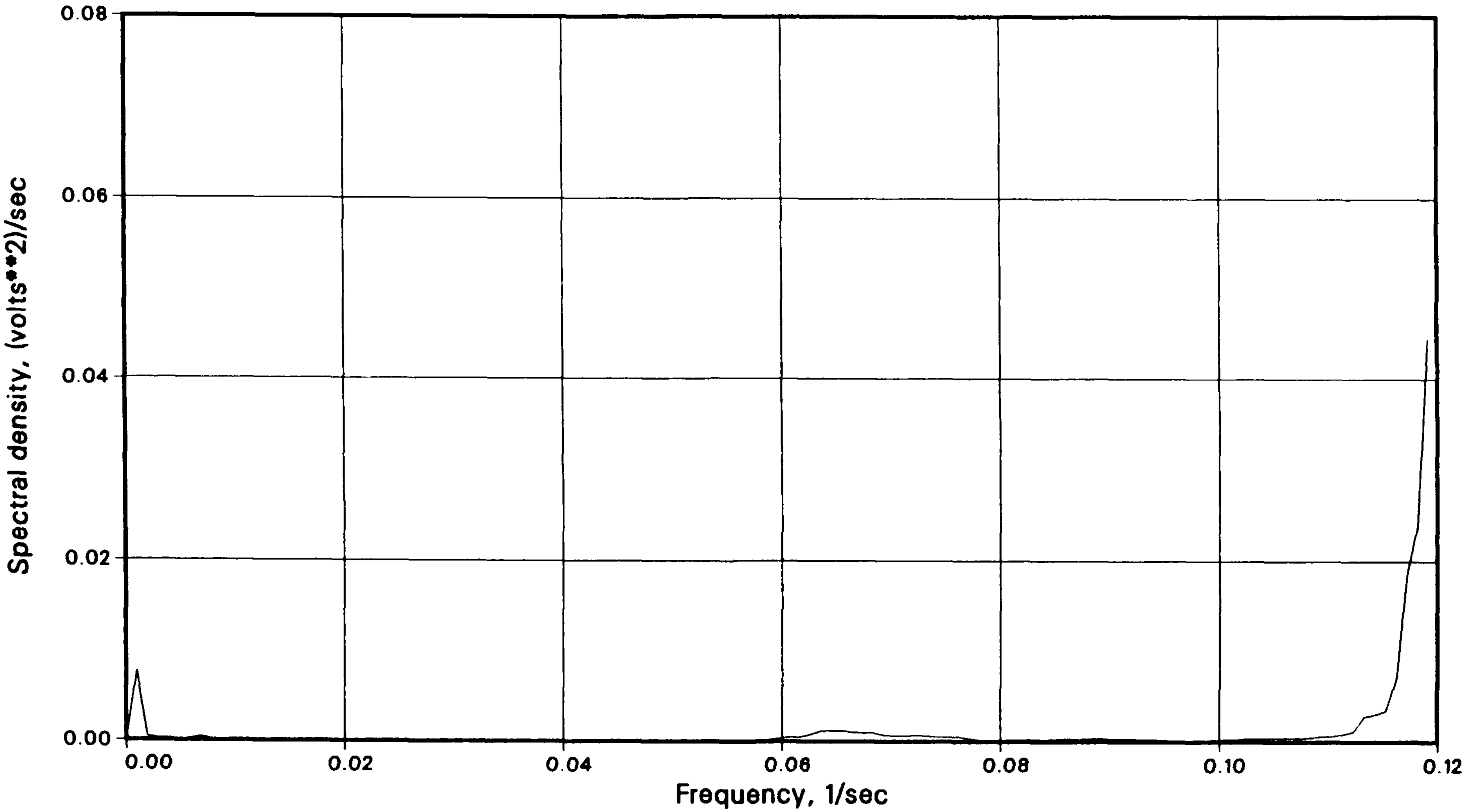

Figure 31. Frequency spectrum of microseisms from 2 August 1985 at 1430

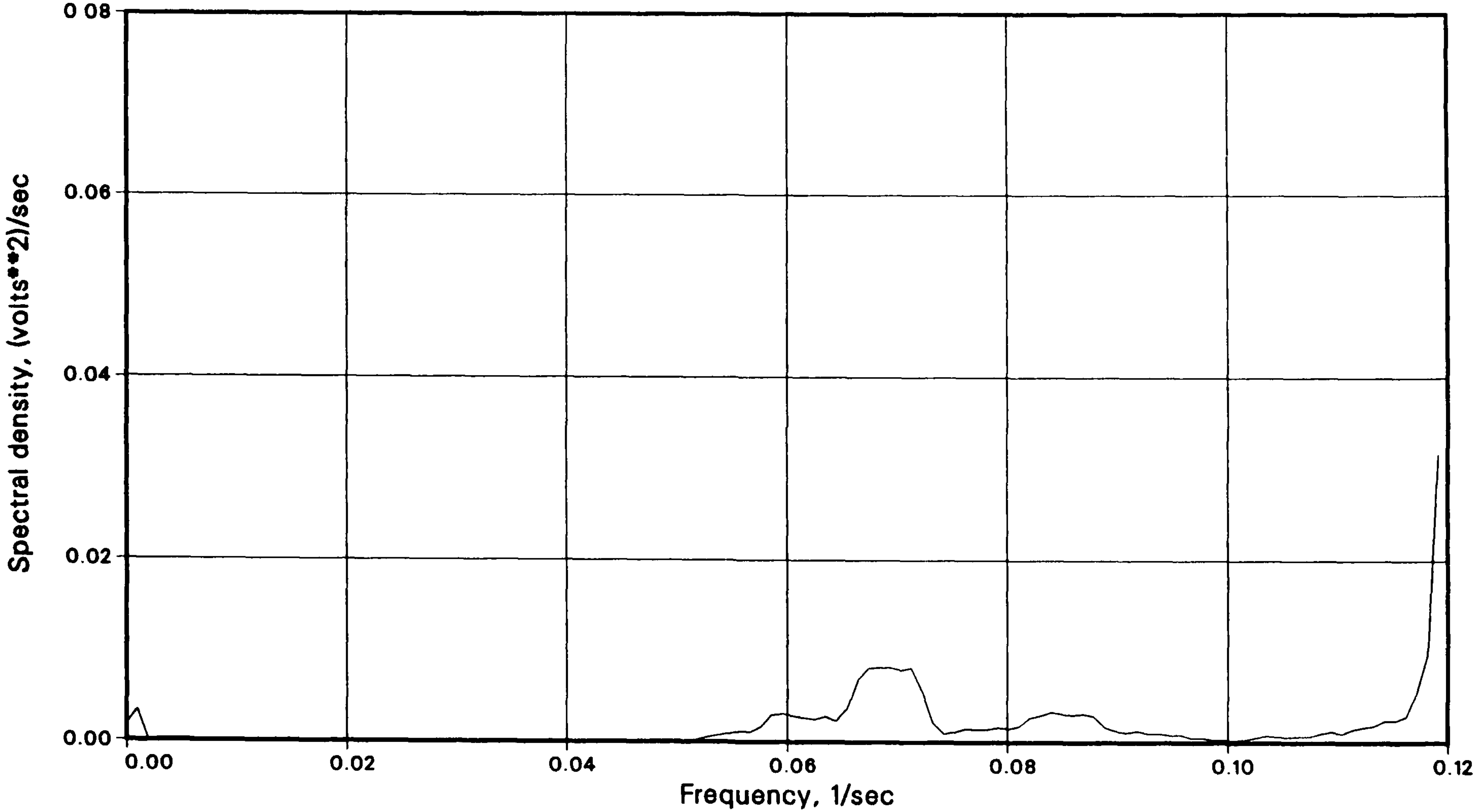

Figure 32. Frequency spectrum of microseisms from 2 August 1985 at 2230

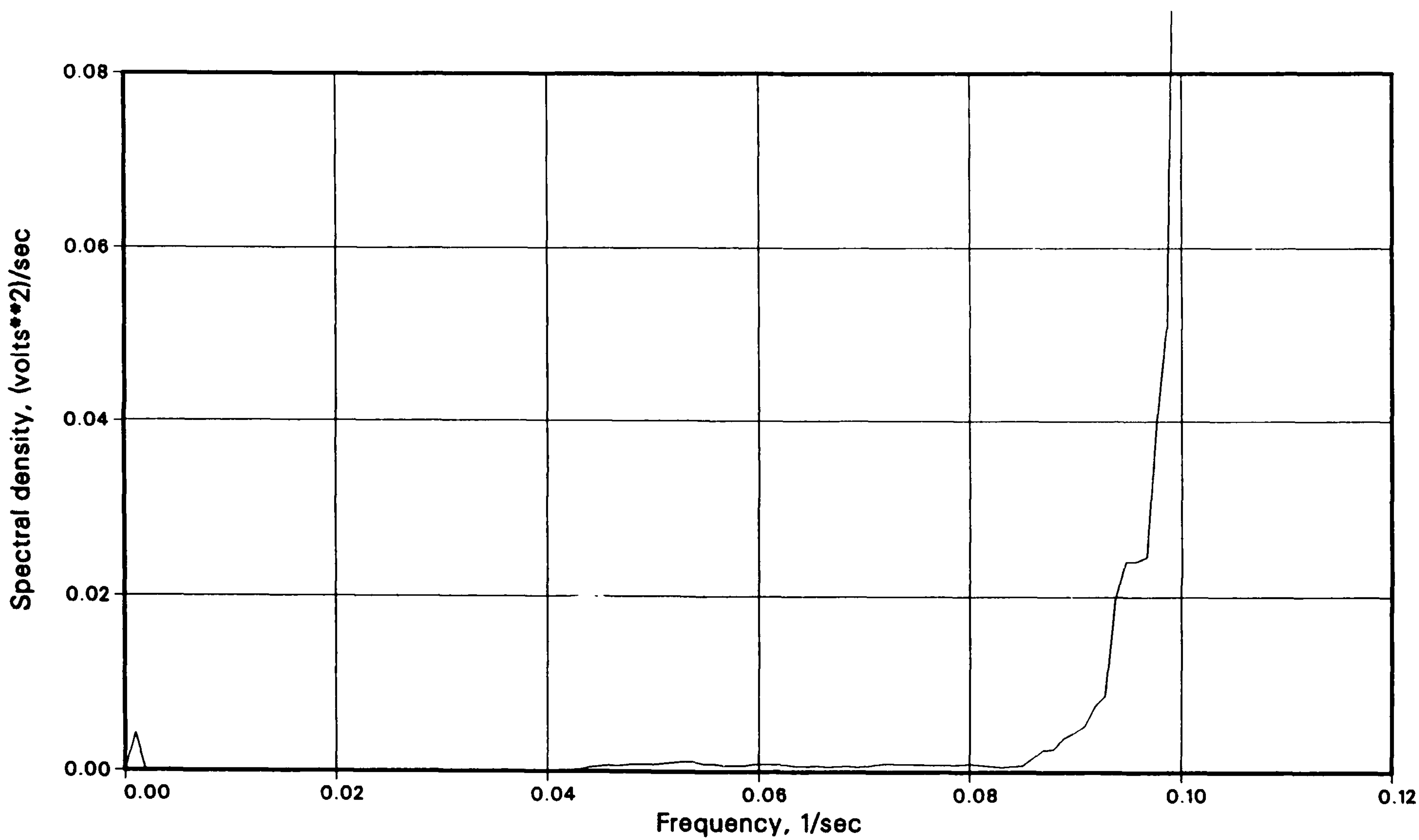

Figure 33. Frequency spectrum of microseisms from 10 March 1986 at 1807

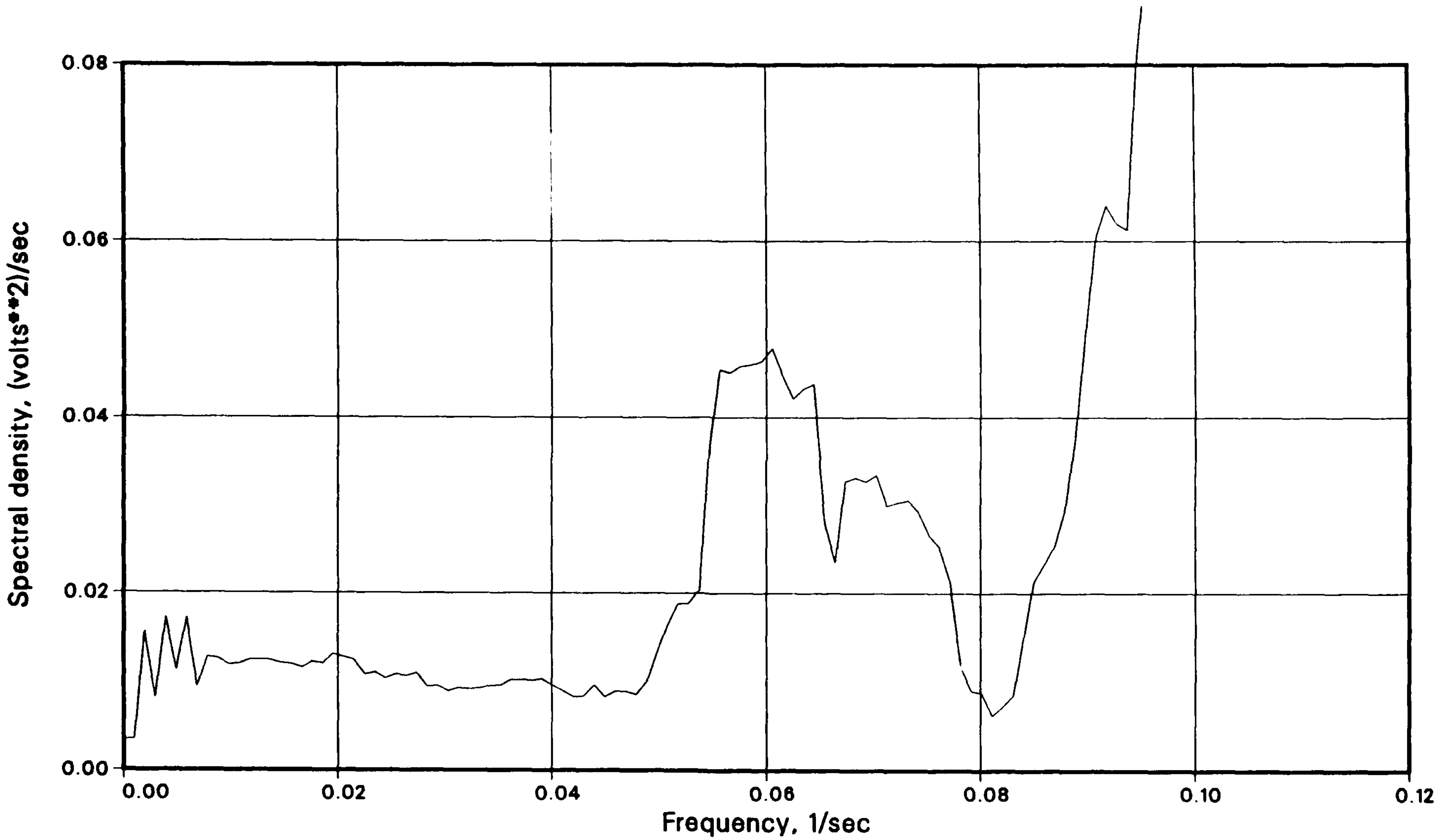

Figure 34. Frequency spectrum of microseisms from 10 March 1986 at 2207

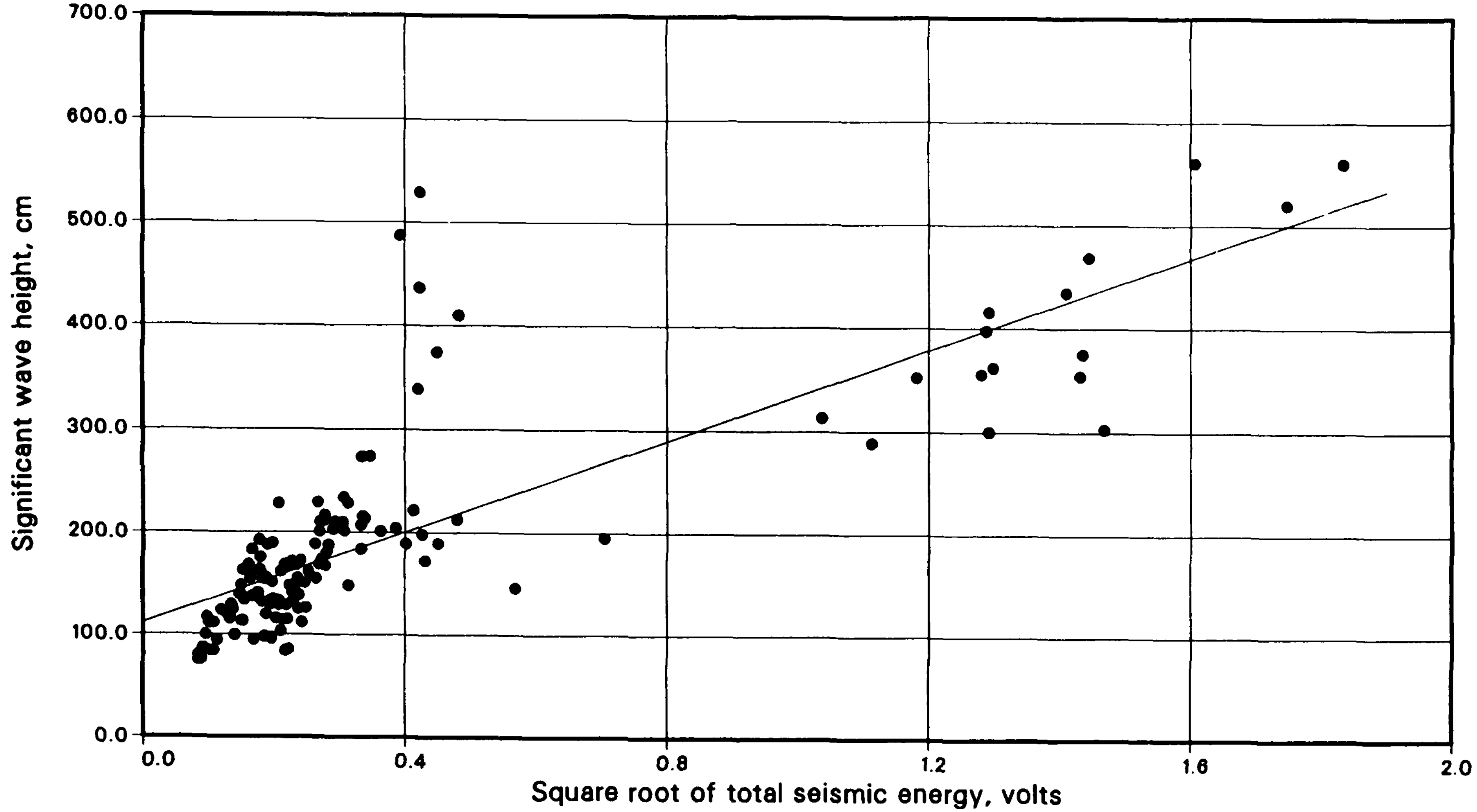

Figure 35. Microseisms versus ocean wave heights at water depth of 230 ft *from July and August 1985 and March and April 1986*

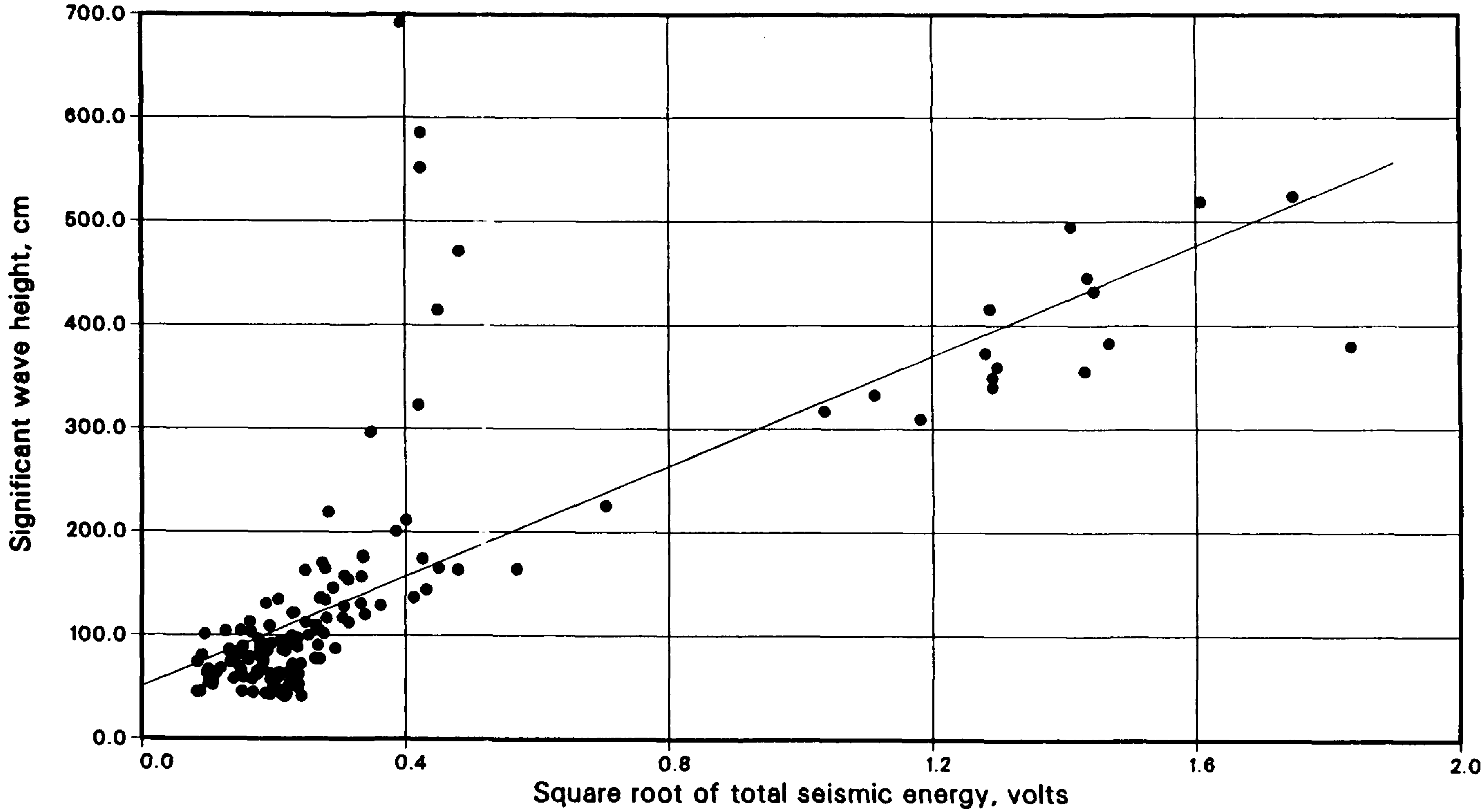

Figure 36. Microseisms versus ocean wave heights at water depth of 52 ft from July and August 1985 and March and April 1986

Appendix A

CORRELATION BETWEEN WAVE HEIGHTS AND ESTIMATES BY SEISMOMETER

Figure A-1 shows the relationship between wave height estimates from the seismometer and significant wave heights at Coquille River (offshore deep water) from SIO. The relationship between wave-height estimates from the seismometer and significant wave heights at Chetco River from OSU is not shown here because the correlation is very poor as can be seen in figures 4 and 5.

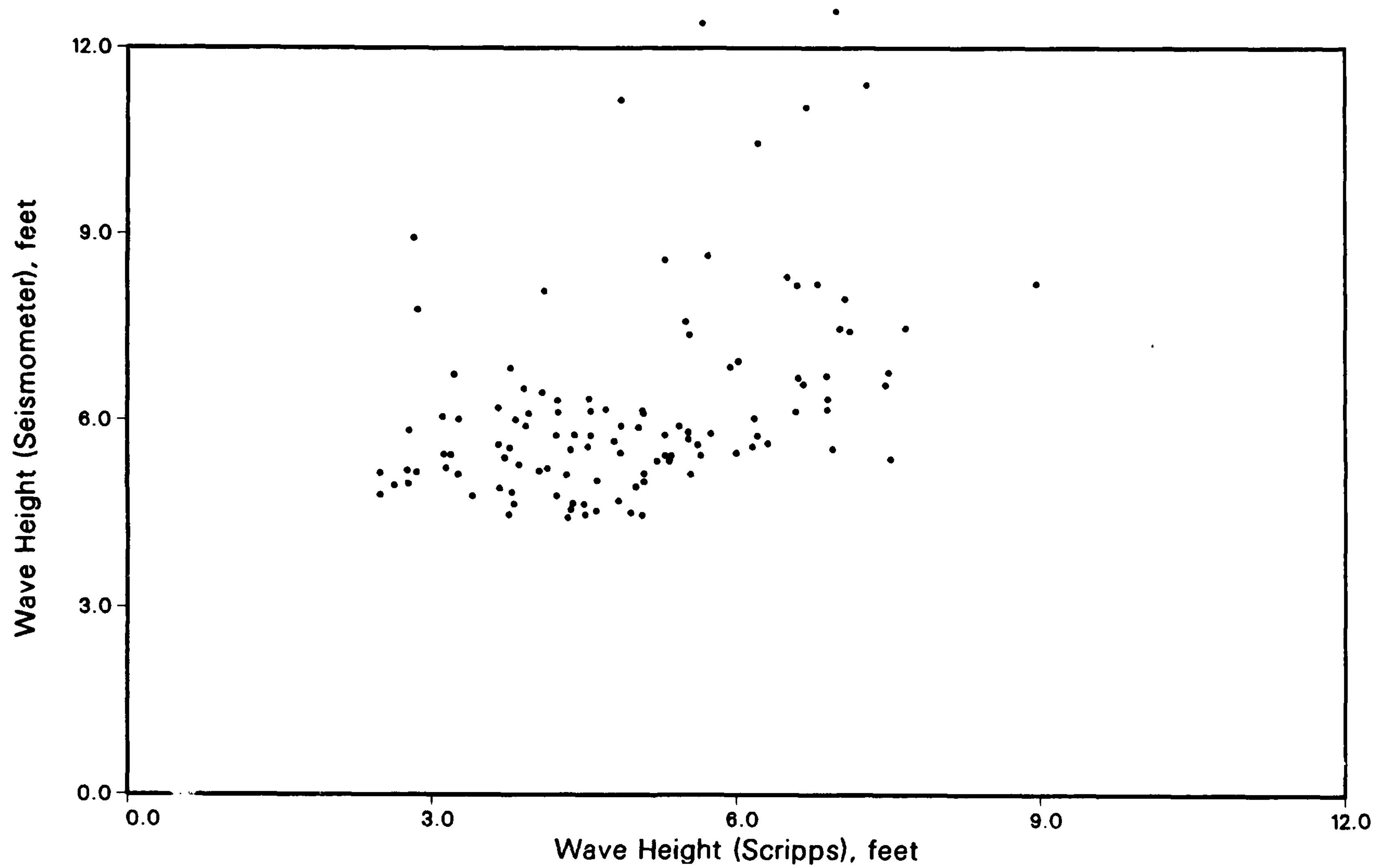

Figure A-1. Correlation between significant wave heights from seismometer and from Scripps (offshore) from July and August 1985